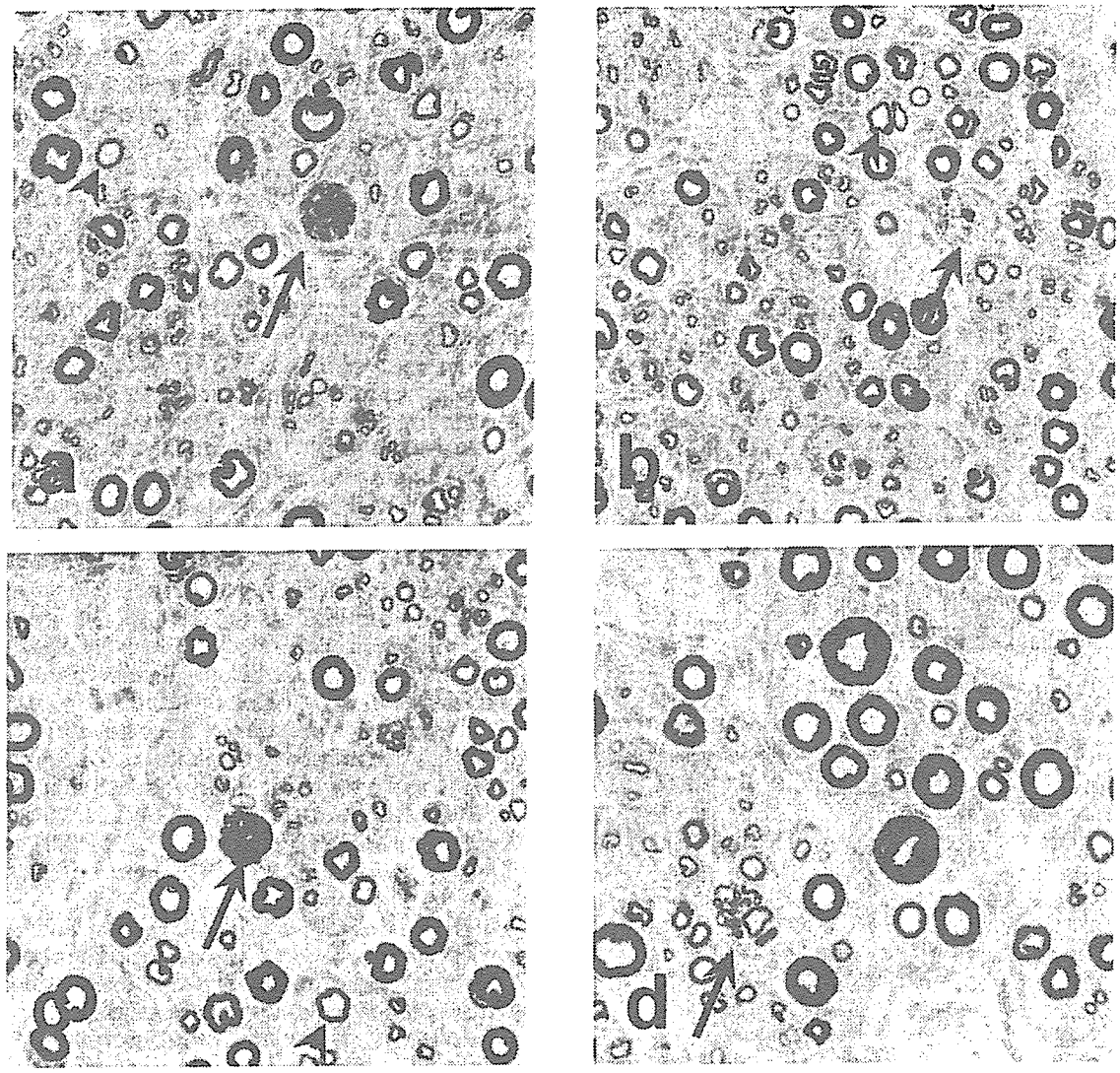

Figure 2 Sural nerve findings of case 1 (**a** and **b**), case 2 (**c**), and case 3 (**d**). Toluidine blue staining (×800). **a** and **b**. Macrophages (*arrows*) containing degenerated myelin sheaths, so-called myelin ovoid. Arrowhead shows thinly myelinated axons. **c**. Arrowhead shows thinly myelinated axons. Myelin globule (*arrow*). **d**. Aggregation of thinly myelinated axons (*arrow*).

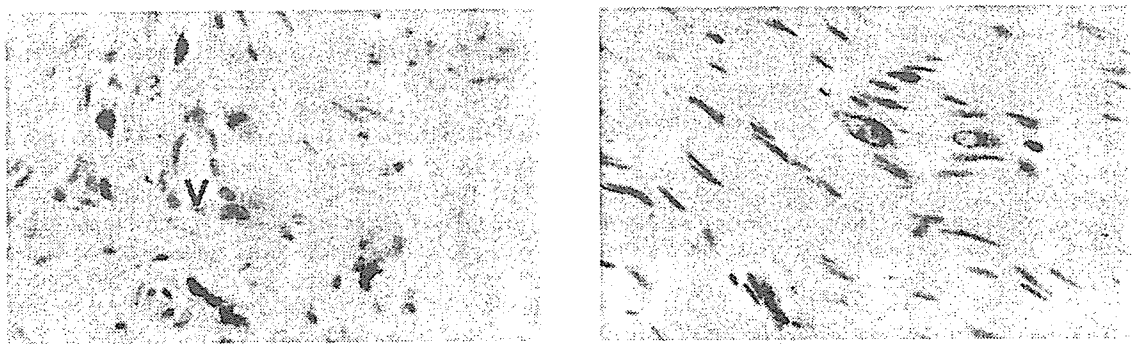

Figure 3 Immunohistochemical findings of the sural nerve of case 2. **a**, Lymphocytes around the nerve fascicles show T-cell markers (CD45R). v, vessel. **b**. Cells found in the nerve fascicles show macrophage markers (CD68).

Table 2 Summary of previously reported cases of HTLV-I–related polyneuropathy

First author	*Year*	*Cases*	*Basic disease*	*NCV/EMG*	*Histopathology*[a]	*Diagnosis/comments*
Arimura	1987	6	HAM	SSEP delay in lower limb	ND	Posterior nerve root/anterior cell lesion?
Said	1988	1	TSP	Axonal/demyelinating PN	Inflammatory neuropathy	Resemblance to CNS lesion in TSP
Funamoto	1989	1	HAM	Axonal/demyelinating PN	De- and remyelination	Slowly progressive myeloneuropathy
Nakazato	1989	2	HAM	Denervation, loss of SNP	Loss of myelinated fibers	Familial HAM with polyneuropathy
Arakawa	1990	1	Carrier	CDP, slow F-wave	ND	Chronic polyradiculoneuropathy
Sugimura	1990	3	HAM	Slight decrease in SCV	Re- and demyelination and globules	Distinct demyelinating process in HAM
Murata m	1990	1	HAM/ATL	Decrease in SCV	Axonal and demyelinating changes	Sensory neuropathy in HAM?
Vernant	1990	5	HAM and PN	ND	Clustered muscular atrophy	PN + myositis with or without HAM
Kohriyama	1992	1	HAM	Delay in MCV/FCV	Axonal and demyelinating changes	Steroid effective; HAM + PN?
Vallat	1993	5	TSP (5/18)	ND	Nonspecific re-, demyelination 3/11[a]	No association with HTLV-I/PN
Bhigjee	1993	6	HAM	Delay in SCV	Axonal/demyelinating change & globule	Primary PN associated with HTLV-I
Kyuno	1993	1	HAM	Delay in SSEP	Neurogenic muscular atrophy	Myopathy
Johkura	1995	1	HAM	Axonal PN, neurogenic	ND	Severe axonal neuropathy in HAM
Kanzaki	1995	1	Carrier	Delay in NCV	Axonal/segmental demyelination; T-cell[b]	PN and myositis in HTLV-I (3% atp-T)
Douen	1997	1	Carrier	Axonal PN, neuromyopathy	Polymyositis (muscle)	PN + myositis + brain lesion in HTLV-I
Hori	1998	1	Smoldering ATL	Delay in FCV and SSEP	ND	Radiculoneuritis + brain lesion in ATL-L
Mitsui	1999	1	HAM, CLL	Abnormal SCV and MCV	Decrease of large myelinated fibers	IgM binding and anti-gangliosides Ab
Yanagihara	1999	1	HAM	Delay in FCV and SSEP	Globular change	Anti-GM1-positive IgG and IgM
Kasahata	2000	1	ATL + HAM	Delay in SSEP	ND	Sensory/motor ataxic PN + meningitis
Nagashima	2001	4	non-HAM	Motor dominant CDP	Demyelination: T-cell	Familial PN without HAM

HAM: HTLV-I–associated myelopathy; ATL: adult T-cell leukemia/lymphoma; PN: peripheral neuropathy; TSP: tropical spastic paraparesis; CLL: chronic lymphocytic leukemia; NCV: nerve conduction velocity; EMG: electromyography; SSEP: short-latency somatosensory evoked potentials; SNP: sensorimotor neuropathy; CDP: chronic demyelinating polyneuropathy; SCV: sensory conduction velocity; FCV: F wave conduction velocity; ND: not described; CNS: central nervous system; Ab: antibody; IgG: immunoglobulin G; IgM: immunoglobulin M; atp-T: atypical T cell.
[a]Sural nerve biopsy.
[b]muscle biopsy.

an HTLV-I–infected 53-year-old female who had a predominantly lower motor neuron disorder. However, the authors could not rule out the possibility of coincidental occurrence of chronic inflammatory demyelinating polyneuropathy. Subsequently, however, similar clinical presentations were reported by Kanzaki *et al* (1995) in an HTLV-I carrier, Douen *et al* (1997) in a patient with myositis, and Hori *et al* (1998) in a patient with the smouldering form of ATLL (Hori *et al*, 1998), thus clearly establishing that polyneuropathy can certainly occur in the setting of HTLV-I infection in the absence of HAM. However, there have been no report of familial cases of polyneuropathy associated with HTLV-I infection. The present study identified four cases over two generations, and supports the proposal that HTLV-I infection is associated with a unique form of familial-associated polyneuropathy. All the patients were intensely seropositive for HTLV-I, but had negative or a lower limit of normal titers in the CSF. General physical examination excluded underlying hematological disorders, and neurological evaluation clearly ruled out the coexistence of HAM. Lack of a high protein level of the spinal fluid ruled out a concomitant association with chronic inflammatory demyelinating disease. Moreover, mutation analyses and the inherited pattern observed in the family tree excluded the inherited peripheral neuropathies (Saito *et al*, 2000). Electrophysiological studies demonstrated a motor dominant chronic demyelinating polyneuropathy without myopathic changes. Although there have been several reports of cases of polymyositis or myopathy complicated by polyneuropathy (Douen *et al*, 1997; Johkura *et al*, 1995; Vernant *et al*, 1990; Yanagihara *et al*, 1999), none of our patients had myositis on muscle biopsy.

Histopathological findings of biopsied sural nerves in HTLV-I infection have been reported as having

decreased numbers of myelinated fibers, axonal degeneration, combined axonal degeneration and segmental demyelination, occurrence of myelin globules, and the presence of myelin ovoid (Funamoto *et al*, 1989; Hori *et al*, 1998; Kanzaki *et al*, 1995; Murata *et al*, 1990; Nakazato *et al*, 1989; Said *et al*, 1988; Sugimura *et al*, 1990; Yanagihara *et al*, 1999). No vasculitis or lymphocytic infiltration has been detected. In our cases, mild-to-moderate loss of myelinated fibers was found in three cases examined and, in addition, features of remyelination were evident in two cases. Myelin globules and myelin ovoids were observed in one case, but axonal degeneration was not evident. Although an inflammatory cell infiltration was not observed in TB staining, a few lymphocytes were found in the endoneurium and perineurial connective tissues by immunostaining. The infiltrating cells expressed the CD45RO T-cell marker and were classified as the CD4 subtype. Peripheral nerves are usually examined using epoxy resin specimens or by the teased fiber method, and immunostaining using lymphocytic markers readily reveals the presence of lymphocytes. To derermine whether the small number of lymphocytes detected in the endo- and perineurium is of significance in HTLV-I polyneuropathy, examination of additional cases will be necessary. CD68-positive macrophages were found in all cases, suggesting the presence of degenerative processes in the nerves.

To begin to investigate possible pathomechanisms involved in HTLV-I–associated familial polyneuropathy, we examined both the viral subtypes of HTLV-I and the HLA alleles of the patients. Recently, nucleotide sequence and phylogenetic analysis of HTLV-I in Japanese patients with HAM/TSP, ATLL, and healthy carriers has revealed a slightly higher incidence of tax subgroup A in patients with HAM/TSP (Yashiki *et al*, 2001). In the present study, we focused our attention on four nucleotide positions in tax which has been shown to serve as useful markers to differentiate tax A and tax B (Yashiki *et al*, 2001). Sequencing of HTLV-I tax gene by PCR method demonstrated that all four patients were infected with HTLV-I tax B subgroup. However, in Japan most HTLV-I infections identified in Hokkaido and Honshu islands are in fact tax B (cosmopolitan B) (Vidal *et al*, 1994), and even the areas where both tax A and tax B are present, tax B is dominant. Therefore, the presence of the HTLV-I subtype tax B in our patients might simply be a reflection of the background population, and may not be related to development of polyneuropathy. Further familial cases are needed to define potential virological factors that might be involved in the development of polyneuropathy.

In our family all patients were female, but as the pedigree shows that there is a female bias in the family, it is unclear if this is significant. The mother of cases 3 and 4 has been free from HTLV-I–associated disorders, but as we have not been able to determine her serological status, it is unknown if she is an asymptomatic carrier. Investigation of the HLA types of all HTLV-I patients has shown significant associations with high immune responsiveness against HTLV-1 *env* (Manns *et al*, 1998; Yashiki *et al*, 2001). Although our patients did not have such alleles as HLA-A26 that have been reported to be associated with ATLL (Manns *et al*, 1998; Yashiki *et al*, 2001), one of them (case 4) does have similar alleles (A24, A33, B54, B39, Cw1, Cw7, DR4, and DR2), which are known to be associated with the risk for development of HAM/TSP. Moreover, in a previously report on two cases with HAM, the HLA haplotype was described as A24, Bw54, CW1, DR4, DQ– (Kawai *et al*, 1989). To determine whether genetic host factors are associated with the development of HTLV-I polyneuropathy, further analysis of the parents of the patient and similar cases will be necessary.

Recently, antibodies against gangliosides have been detected in the patients who have developed polyneuropathy associated with HTLV-I (Mitsui *et al*, 1999; Yanagihara *et al*, 1999). The pathogenetic importance of antiganglioside antibodies in sensory and motor neuropathy has been established in non-HTLV-I–infected patients (Oka *et al*, 1996; Pestronk *et al*, 1990; Sadiq *et al*, 1990; Umehara *et al*, 1997). In this study, among the family members (see Figure 4), we have examined anti-HTLV-I antibody titer only in cases 1, 2, 3, 4, and II-1. As cases I-1, I-2, II-4, and II-5 were deceased and cases II-2, III-3, and III-4 were healthy, we had no information relating to their blood analysis. We excluded case II-1 who had relatively high titers against HTLV-I (1,024×), because we did not have detailed clinical information on this patient. We hypothesized that high antibody titers against HTLV-I virus proteins could result in cross reactions against peripheral nerve glycolipids and/or proteins, resulting in an autoimmune response and may have caused the disease. This hypothesis is supported by the fact that most of patients

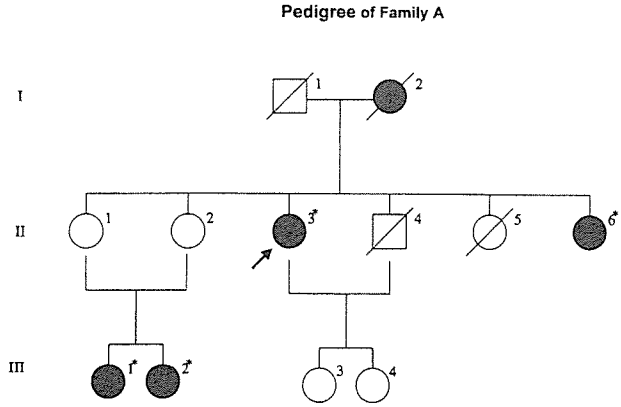

Figure 4 Pedigree of Family A. I-1: death of esophageal cancer; I-2: death of malignant lymphoma. II-1: suffering from sick sinus syndrome; II-3: case 1; II-4: sudden death; II-5: death of subarachnoid hemorrhage; II-6: case 2. III-1: case 3; III-2: case 4. *Cases examined.

with HTLV-I–associated polyneuropathy recovered or improved with steroid therapy. However, further studies will be necessary to clarify this and should help in our understanding of the pathogenesis of this form of familial polyneuropathy.

Patients and methods

Case histories

Clinical summaries of the four patients are shown in Table 1. The family pedigree (Figure 4) shows that the first generation individuals (I-1, -2) were born and spent their entire lives in the city in Hokkaido in Japan, where the average seropositivity for HTLV-I antibody of adult blood donors measured in 1984 was the second lowest (1.0%) in Japan (Tajima, 1990). The patients' mother (I-2) died of malignant lymphoma but apparently also developed numbness of the feet late in life.

Case 1 (II-3, the proband), a 61-year-old woman had a history of recurrent uveitis and hearing difficulties since childhood. At age 18, she noticed a gait disturbance and hoarseness that was followed by the gradual development of a distal sensorimotor abnormality, generalized edema, and exertional dyspnea. At age 54, she was diagnosed with a thyroid cancer by lymph node biopsy, which disclosed metastatic papillary carcinoma. After surgery and subsequent treatment with thyroxin, she noticed the progression of a sensorimotor paresis of the extremities with rectourinary disturbances. Seven years later, her thyroid cancer relapsed and required further surgery but not chemotherapy. On admission she was found to be seropositive for HTLV-I. Neurological examination demonstrated a sensory and motor paresis with pain and numbness affecting mainly the lower extremities with urinary urgency. Deep tendon reflexes were decreased or negative without pyramidal or any pathological signs. Neuroradiological studies, including brain and spinal cord magnetic resonance imaging (MRI) and skeletal muscle computed tomography (CT), revealed no metastatic mass lesions or abnormal enhancing lesions in the CNS, whereas moderate amyotrophy with fatty replacement was noticed mainly in the muscles of the lower extremities.

Case 2 (II-6) was a 53-year-old woman and the second younger sister of the proband. At age 43, she had a hysterectomy following a diagnosis of uterine cancer but did not receive blood transfusions or any postoperative chemotherapy. Three years later, she developed hoarseness and transient numbness of the lower extremities. Examination revealed generalised arthralgia, paresthesia, urinary urgency, and unsteady gait. Muscle weakness with numbness was noted in the lower extremities. Pyramidal signs and pathological reflexes were negative. Tumor markers and general radiological studies for the recurrence of her gynecological malignancy were negative.

Case 3 (III-1) was the first niece of the proband, a 52-year-old woman who had been suffering from several minor illness, including keratoconjunctivitis and hemolytic diathesis during her childhood, migraine and chronic hepatitis (hepatitis B virus [HBV] antibody positive) since the second decade of life, and paresthesias with pain in the calf muscle and weakness of extremities since her late teenage years. On the initial examination in our hospital at age 52, she presented with a mild kyphosis of the spine, distal dominant sensorimotor paresis with moderate amyotrophy and positive Barre signs in the legs. Deep tendon reflexes were decreased and her gait was unsteady. There was no urinary disturbance. Routine laboratory examination, including blood chemistry, peripheral blood count, and autoantibodies, was unremarkable except for high serum titer of HTLV-I and a positive HBV antibody titer.

Case 4 (III-2), the younger sister of case 3, noticed an unsteady gait, numbness of the feet, and headache at age of around 45 years. She had a history of pulmonary tuberculosis in her adolescence. At age 50, she tested seropositive for hepatitis C virus and also HTLV-I. Neurologically, she was noted to have paretic gait with mild hyperactive patellar tendon reflexes, painful paresthesia below the knee joint, mild motor weakness of legs, and subjective urinary urgency. Chest x-ray showed that the left lung was shrunken as a result of a previous lobectomy for tuberculosis, and moderate hypoventilation was confirmed by a spirogram. Neuroradiological studies were unremarkable except for moderate muscle atrophy in the lower extremities.

Cytological examination of CSF in all four patients revealed neither a high protein level nor atypical or malignant cells in the CSF.

Virological studies

Viral antibody titers for HTLV-I were examined by the Kishimoto Clinical Laboratory (Tomakomai, Japan) using the particle agglutination (PA) method. Serological assays for HIV-1 and-2 and other conventional viruses were examined in sera and CSF of all four patients.

HLA analysis

Serological typing for HLA of the patients was examined by the SRL Inc. (Tokyo, Japan) using a usual procedure.

Mutational analysis

Heteroduplex analysis and single strand conformation polymorphism analysis (Nelis *et al.* 1996) were performed to detect the mutation in the PMP22 gene and the P0 gene, which have been associated with the autosomal dominant type of Charcot-Marie-Tooth neuropathies (Keller and Chance, 1999). Primer sets used for PCR amplification of PMP22 and P0 genes were as previously described (Nelis *et al*, 1994).

Electrophysiological studies
Routine motor/sensory NCSs, studies of F-wave and SSEPs, and needle EMG were performed using standard procedures.

Pathological examination
Histological and immunohistochemical analyses were carried out on biopsies of skin, muscle (hamstring muscle), and sural nerves of all patients. Materials were divided into two: one for paraffin sections, the other for epoxy resin preparations. Paraffin sections including hematoxylin-eosin (H&E) and Elastica van Gieson staining with Masson trichrome were used for routine histological examination and for immunohistochemistry. Antibodies used for immunostaining were CD3 (Dako, Glostrup, Denmark), CD45RO (UCHL-1; Dako), CD4 (Nichirei, Tokyo, Japan), CD8 (Nichirei), CD20 (L-26; Dako), and CD68 (Dako). Epoxy resin preparations were stained with TB.

Nucleotide sequencing analysis
DNA samples were extracted from white blood cells of all patients, and were analyzed by the method by Furukawa *et al* (2000). PCR was performed to amplify the tax region of the provirus using primer sets PX01+ and PX02− and amplified products were extracted and purified from agarose gels. Purified DNAs were sequenced with the primers PX01+, TaxF 286, TaxF 566, and PX01p and analyzed as previously described (Furukawa *et al*, 2000).

References

Arakawa K, Umezaki H, Noda S, Itoh H (1990). Chronic polyradiculoneuropathy associated with human T-cell lymphotropic virus type I infection. *J Neurol Neurosurg Psychiatry* **53**: 358–359.

Arimura K, Rosales R, Osame M, Igata A (1987). Clinical electrophysiologic studies of HTLV-I-associated myelopathy. *Arch Neurol* **44**: 609–612.

Bhigjee AI, Bill PL, Wiley CA, Windsor IM, Matthias DA, Amenomori T, Wachsman W, Moorhouse D (1993). Peripheral nerve lesions in HTLV-I associated myelopathy (HAM/TSP). *Muscle Nerve* **16**: 21–26.

Cabrera ME, Gray AM, Cartier L, Araya F, Hirsh T, Ford AM, Greaves MF (1991). Simultaneous adult T-cell leukemia/lymphoma and sub-acute polyneuropathy in a patient from Chile. *Leukemia* **5**: 350–353.

Douen AG, Pringle CE, Guberman A (1997). Human T-cell lymphotropic virus type 1 myositis, peripheral neuropathy, and cerebral white matter lesions in the absence of spastic paraparesis. *Arch Neurol* **54**: 896–900.

Funamoto K, Takada K, Inoue K, Sawada Y, Araga S, Takahashi K (1989). Peripheral nerve involvement in HTLV-I-associated myelopathy: report of a case. *Jpn J Med* **28**: 762–764.

Furukawa Y, Yamashita M, Usuku K, Izumo S, Nakagawa M, Osame M (2000). Phylogenetic subgroups of human T cell lymphotropic virus (HTLV) type I in the tax gene and their association with different risks for HTLV-I-associated myelopathy/tropical spastic paraparesis. *J Infect Dis* **182**: 1343–1349.

Gessain A, Barin F, Vernant JC, Gout O, Maurs L, Calender A, de The G (1985). Antibodies to human T-lymphotropic virus type-I in patients with tropical spastic paraparesis. *Lancet* **2**: 407–410.

Hori T, Tsuboi Y, Kiyose H, Kamei H, Nishimaru K, Yamada T (1998). [A case of HTLV-I associated polyradiculoneuropathy and cerebral white matter lesions with smouldering type adult T cell leukemia.] *Rinsho Shinkeigaku* **38**: 645–648.

Johkura K, Matsumoto S, Kurakoshi Y, Hasegawa O, Kuroiwa Y (1995). HTLV-I associated myelopathy with severe polyneuropathy. *Neurol Med (Tokyo)* **43**: 239–243.

Johnson JM, Harrod R, Franchini G (2001). Molecular biology and pathogenesis of the human T-cell leukaemia/lymphotropic virus type-1 (HTLV-1). *Int J Exp Pathol* **82**: 135–147.

Kanzaki A, Yabuki S, Shirabe T (1995). [HTLV-I-associated neuropathy.] *No To Shinkei* **47**: 497–501.

Kasahata N, Kawamura M, Shiota J, Miyazawa Y, Suzuki Y, Sugita K (2000). [A case of acute type adult T cell leukemia and human T-lymphotropic virus type I associated myelopathy who presented meningitis and polyradiculoneuropathy and improved with steroid treatment.] *No To Shinkei* **52**: 1003–1006.

Kawai H, Nishida Y, Takagi M, Nakamura K, Masuda K, Saito S, Shirakami A (1989). HTLV-I-associated myelopathy with adult T-cell leukemia. *Neurology* **39**: 1129–1131.

Keller MP, Chance PF (1999). Inherited peripheral neuropathy. *Semin Neurol* **19**: 353–362.

Kohriyama T, Kohriyama S, Katayama S, Yamamura Y, Nakamura S (1992). HTLV-I associated myelopathy (HAM) accompanied by corticosteroid-responsive encephalopathy and neuropathy. A case report. *Neurol Med (Tokyo)* **37**: 143–148.

Kuroda Y, Nakata H, Kakigi R, Oda K, Shibasaki H, Nakashiro H (1989). Human neurolymphomatosis by adult T-cell leukemia. *Neurology* **39**: 144–146.

Kyuno K, Ito H, Hasegawa H, Saito T, Kowa, H (1993). [A case of flaccid paraplegia associated with HTLV-I infection.] *Rinsho Shinkeigaku* **33**: 754–758.

Manns A, Hanchard B, Morgan OS, Wilks R, Cranston B, Nam JM, Blank M, Kuwayama M, Yashiki S, Fujiyoshi T, Blattner W, Sonoda S (1998). Human leukocyte antigen class II alleles associated with human T-cell lymphotropic virus type I infection and adult T-cell leukemia/lymphoma in a Black population. *J Natl Cancer Inst* **90**: 617–622.

Mitsui Y, Kusunoki S, Hiruma S, Akamatsu M, Kihara M, Hashimoto S, Takahashi M (1999). Sensorimotor polyneuropathy associated with chronic lymphocytic leukemia, IgM antigangliosides antibody and human T-cell leukemia virus I infection. *Muscle Nerve* **22**: 1461–1465.

Murat M, Mizusawa H, Kanazawa I, Yazawa T, Uchida Y (1990). [An autopsy case of HTLV-I associated myelopathy (HAM) with adult T-cell leukemia (ATL).] *Rinsho Shinkeigaku* **30:** 754–759.

Nagai M, Jacobson S (2001). Immunopathogenesis of human T cell lymphotropic virus type I-associated myelopathy. *Curr Opin Neurol* **14:** 381–386.

Nakano S, Ohnishi A, Oishi T, Murai Y, Nagata K (1991). [A case of adult T cell leukemia/lymphoma with motor and sensory polyneuropathy.] *Rinsho Shinkeigaku* **31:** 853–857.

Nakazato O, Mori T, Okajima T (1989). Sural nerve pathology in HTLV-I associated myelopathy. In: *HTLV-I and the nervous system*. Roman GC, Vermant JC, Osame M (eds). New York: Alan R. Liss, pp 269–274.

Nelis E, Timmerman V, De Jonghe P, Vandenberghe A, Pham-Dinh D, Dautigny A, Martin JJ, Van Broeckhoven C (1994). Rapid screening of myelin genes in CMT1 patients by SSCP analysis: identification of new mutations and polymorphisms in the P0 gene. *Hum Genet* **94:** 653–657.

Nelis E, Warner LE, Vriendt ED, Chance PF, Lupski JR, Van Broeckhoven C (1996). Comparison of single-strand conformation polymorphism and heteroduplex analysis for detection of mutations in Charcot-Marie-Tooth type 1 disease and related peripheral neuropathies. *Eur J Hum Genet* **4:** 329–333.

Oka N, Kusaka H, Kusunoki S, Tsuda H, Kaji R, Imai T, Akiguchi I, Kimura J (1996). IgM M-protein with antibody activity against gangliosides with disialosyl residue in sensory neuropathy binds to sensory neurons. *Muscle Nerve* **19:** 528–530.

Okamura S, Niho Y, Mitsui T, Kikuchi M (1984). Adult T-cell leukemia and polyneuropathy. A case report. *Nippon Ketsueki Gakkai Zasshi* **47:** 1344–1350.

Osame M, Usuku K, Izumo S, Ijichi N, Amitani H, Igata A, Matsumoto M, Tara M (1986). HTLV-I associated myelopathy, a new clinical entity. *Lancet* **1:** 1031–1032.

Pestronk A, Chaudhry V, Feldman EL, Griffin JW, Cornblath DR, Denys EH, Glasberg M, Kuncl RW, Olney RK, Yee WC (1990). Lower motor neuron syndromes defined by patterns of weakness, nerve conduction abnormalities, and high titers of antiglycolipid antibodies. *Ann Neurol* **27:** 316–326.

Sadiq SA, Thomas FP, Kilidireas K, Protopsaltis S, Hays AP, Lee KW, Romas SN, Kumar N, van den Berg L, Santoro M (1990). The spectrum of neurologic disease associated with anti-GM1 antibodies. *Neurology* **40:** 1067–1072.

Said G, Goulon-Goeau C, Lacroix C, Feve A, Descamps H, Fouchard M (1988). Inflammatory lesions of peripheral nerve in a patient with human T-lymphotropic virus type I–associated myelopathy. *Ann Neurol* **24:** 275–277.

Saito S, Ota S, Yamada E, Inoko H, Ota M (2000). Allele frequencies and haplotypic associations defined by allelic DNA typing at HLA class I and class II loci in the Japanese population. *Tissue Antigens* **56:** 522–529.

Sugimura K, Takahashi A, Watanabe M, Mano K, Watanabe H (1990). Demyelinating changes in sural nerve biopsy of patients with HTLV-I-associated myelopathy. *Neurology* **40:** 1263–1266.

Tajima K (1990). The 4th nation-wide study of adult T-cell leukemia/lymphoma (ATL) in Japan: estimates of risk of ATL and its geographical and clinical features. The T- and B-cell Maliganancy Study Group. *Int J Cancer* **45:** 237–243.

Umehara F, Kore-Eda Y, Arime T, Kubota R, Arimura K, Osame M (1997). Chronic sensory ataxic neuropathy and ophthalmoplegia with oculomotor nerve hypertrophy associated with IgM antibodies against gangliosides containing disialosyl groups. *J Neurol Neurosurg Psychiatry* **62:** 673–674.

Vallat JM, Dumas M, Grunitzky EK, Akani F, Diop G, Ramiandrisoa H, Denis F (1993). Lack of association between peripheral neuropathy and HTLV-I infection in West Africa. Epidemiological, serological and nerve biopsy study. *J Neurol Sci* **119:** 141–145.

Vernant JC, Bellance R, Buisson GG, Havard S, Mikol J, Roman G (1990). Peripheral neuropathies and myositis associated to HTLV-I infection in Martinique. In: *Human retrovirology: HTLV*. Blattner WA (ed). New York, Raven Press, pp 225–235.

Vidal AU, Gessain A, Yoshida M, Mahieux R, Nishioka K, Tekaia F, Rosen L, De The G (1994). Molecular epidemiology of HTLV type I in Japan: evidence for two distinct ancestral lineages with a particular geographical distribution. *AIDS Res Hum Retroviruses* **10:** 1557–1566.

Yamaguchi K, Takatsuki K (1993). Adult T cell leukaemia-lymphoma. *Baillieres Clin Haematol* **6:** 899–915.

Yanagihara C, Ihara M, Nishimura Y, Oka N (1999). [A case of anti-GM1 antibody positive HTLV-I associated myelopathy (HAM) with polyneuropathy.] *Rinsho Shinkeigaku* **39:** 971–975.

Yashiki S, Fujiyoshi T, Arima N, Osame M, Yoshinaga M, Nagata Y, Tara M, Nomura K, Utsunomiya A, Hanada S, Tajima K, Sonoda S (2001). HLA-A*26, HLA-B*4002, HLA-B*4006, and HLA-B*4801 alleles predispose to adult T cell leukemia: the limited recognition of HTLV type 1 tax peptide anchor motifs and epitopes to generate anti-HTLV type 1 tax CD8(+) cytotoxic T lymphocytes. *AIDS Res Hum Retroviruses* **17:** 1047–1061.

Yoshida M (2001). Multiple viral strategies of HTLV-1 for dysregulation of cell growth control. *Annu Rev Immunol* **19:** 475–496.

Available online at www.sciencedirect.com
SCIENCE DIRECT®
ELSEVIER
Biochemical and Biophysical Research Communications 327 (2005) 242–251
BBRC
www.elsevier.com/locate/ybbrc

Establishment of an immunoscreening system using recombinant VP1 protein for the isolation of a monoclonal antibody that blocks JC virus infection

Chizuka Henmi[a], Hirofumi Sawa[a,b,*], Hiroshi Iwata[a], Yasuko Orba[a], Shinya Tanaka[a], Kazuo Nagashima[a]

[a] *Laboratory of Molecular and Cellular Pathology, Hokkaido University School of Medicine, CREST, JST, Sapporo 060-8638, Japan*
[b] *21st Century COE Program for Zoonosis, Graduate School of Medicine, Hokkaido University, Japan*

Received 15 November 2004
Available online 13 December 2004

Abstract

Polyomavirus JC (JCV) infection causes the fatal human demyelinating disease, progressive multifocal leukoencephalopathy. Although the initial interaction of JCV with host cells occurs through direct binding of the major viral capsid protein (VP1) with cell-surface molecules possessing sialic acid, these molecules have not yet been identified. In order to isolate monoclonal antibodies which inhibit attachment of JCV, we established an immunoscreening system using virus-like particles consisting of the VP1. Using this system, among monoclonal antibodies against the cell membrane fraction from JCV-permissive human neuroblastoma IMR-32 cells, we isolated a monoclonal antibody designated as 24D2 that specifically inhibited attachment and infection of JCV to IMR-32 cells. The antibody 24D2 recognized a single molecule of around 60 kDa in molecular weight in the IMR-32 membrane fraction. Immunohistochemical staining with 24D2 demonstrated immunoreactivity in the cell membrane of JCV-permissive cell lines and glial cells of the human brain. These results suggested that the molecule recognized by 24D2 plays a role in JCV infection, and that it might participate as a receptor or a co-receptor in JCV attachment and entry into the cells.

Keywords: JC virus; VP1; VLP; Monoclonal antibody; PML

JC virus (JCV), which belongs to the polyomavirus family of non-enveloped DNA viruses, is known to be a causative agent of the progressive multifocal leukoencephalopathy (PML), a demyelinating disease of the central nervous system (CNS). PML affects mainly immunosuppressed patients, such as those with acquired immunodeficiency syndrome (AIDS) or following organ transplantation, and has increased in prevalence with the spread of transplantations and AIDS. However, there is still no effective treatment for PML. The major target cells of JCV infection in the CNS are the glial cells, such as oligodendrocytes and astrocytes [1]. The first step in the establishment of JCV infection is attachment of the viral capsid to receptors on host cells.

The capsid of JCV is composed of three capsid proteins, VP1, VP2, and VP3. VP1, encoded by the late region of JCV, is the major capsid protein that forms the outer surface of the virion. It has been reported that recombinant VP1 derived from *Escherichia coli* or insect cells can form virus-like particles (VLPs), and exhibit cellular attachment and intracytoplasmic trafficking similar to those of JCV virions [2–5]. In addition, VP1 has been reported to play a major function in the attachment of JCV to cells as the anti-VP1 antibody suppresses viral entry into cells and subsequent infection

* Corresponding author. Fax: +81 11 706 7806.
E-mail address: h-sawa@patho2.med.hokudai.ac.jp (H. Sawa).

0006-291X/$ - see front matter © 2004 Elsevier Inc. All rights reserved.
doi:10.1016/j.bbrc.2004.11.158

[5]. The cellular receptor molecule for JCV is unknown, but it has been reported to be an N-linked glycoprotein containing α2–6-linked sialic acids, based on the observation that α2–6-specific sialidase inhibits infection of glial cells by JCV. In addition, treatment of permissive cells with tunicamycin, which removes N-linked oligosaccharides, was shown to inhibit JCV infection in vitro [6]. These findings indicate that the interaction between the major structural protein VP1 and sialic acids is critical for JCV infectivity. However, non-enveloped viruses are unable to fuse with the cell lipid membrane bilayer, and their internalization is thought to require a specific entry receptor. Furthermore, it has been reported that infectious entry of JCV requires a ligand-inducible signal that is inhibited by genistein, a protein–tyrosine kinase inhibitor [7]. The mechanisms by which JCV binds and enters host cells and the molecules involved are not yet completely understood.

The mouse polyomavirus (PyV) is also known to bind to the sialic acid residues of a not yet identified receptor. Recently, antibodies to α4β1 integrin have been shown to partially block PyV infection. Therefore, the integrin has been suggested to act as an entry receptor for the early stages of PyV infection in fibroblasts [8].

Antibodies that react with cell-surface molecules have important applications as therapeutic agents and in the identification of viral receptors. Therefore, we attempted to isolate monoclonal antibodies to molecules on JCV-permissive cells. To isolate the monoclonal antibodies against the cell-surface molecules related to JCV infection on permissive cells, we developed an immunoscreening method and attempted to isolate blocking antibodies against JCV infection.

Using this immunoscreening system, we isolated a monoclonal antibody that recognizes the cellular-surface molecules related to JCV infection. The antibody also significantly blocked the attachment and subsequent infection of JCV. The molecule recognized by this antibody was considered to participate in virus infection, suggesting that this molecule acts as a virus receptor and/or a co-receptor. Here, we report the successful isolation and characterization of a monoclonal antibody with blocking activities toward JCV infection.

Materials and methods

Cells and antibodies

The human neuroblastoma cell line, IMR-32 (JCRB 9050), human embryonic kidney cell line, HEK293 (JCRB 9068), and human cervical carcinoma cell line, HeLa (JCRB 9004), were provided by the Health Science Research Resources Bank (Osaka, Japan). The African green monkey kidney cell line, COS-7 (#CRL 1651), was obtained from the American Type Culture Collection (Rockville, MD), and the human glial cell line, SVG-A, was kindly provided by Dr. Atwood [9]. All cell lines were maintained in Dulbecco's minimal essential medium (DMEM) supplemented with 10% heat-inactivated fetal bovine serum (FBS) and antibiotics (penicillin and streptomycin, Sigma, St. Louis, MO) in 5% CO_2 at 37 °C. The anti-VP1 polyclonal antibody and anti-agnoprotein antibodies were prepared as described previously [5,10]. The anti-SV40T-antigen, which is known to be cross-reactive with anti-JCV T-antigen (Ab-2) monoclonal antibody, was purchased from Calbiochem (San Diego, CA). Anti-actin monoclonal antibody was purchased from Chemicon (Temecula, CA). Anti-GFAP polyclonal antibody (Nichirei, Tokyo, Japan), anti-synaptophysin monoclonal antibody (Dako, Japan), and anti-CA-2 polyclonal antibody (The Binding Site, Birmingham, UK) were prepared commercially. A mouse IgM-isotype control antibody was obtained from Sigma (St. Louis, MO).

JC virus and recombinant virus-like particles

Preparation of native JCV was performed as described previously [5]. Briefly, cell lysates from the JCV-producing cell line, JCI cells, were harvested, subjected to repeated freeze–thaw cycles, and then treated with 0.05 mg/ml neuraminidase type I (Sigma) at 37 °C for 16 h. After treatment with neuraminidase, samples were incubated at 56 °C for 30 min and centrifuged at 1000*g* for 10 min. The viral titer of virus-containing supernatant was quantified by hemagglutination (HA) assay and stored at −80 °C until use.

The preparation of virus-like particles (VLPs) was performed as described previously [5]. Briefly, the VP1 gene of JCV from pBR-Mad1 [11] was subcloned into the prokaryotic expression vector pET15-b (Novagen, Madison, WI). The plasmid was transformed into *E. coli*, BL21 (DE3)/pLys (Stratagene, La Jolla, CA). The expression of VP1 was induced with 1.0 mM isopropyl-β-D-thiogalactopyranoside (IPTG) for 4 h at 30 °C, and the mixture was centrifuged at 4000*g* for 10 min. The cell pellet was resuspended in reassociation buffer (10 mM Tris–HCl, pH 7.5, 150 mM NaCl, and 1.0 mM $CaCl_2$) containing 1 mg/ml lysozyme, kept on ice for 30 min, and then sodium deoxycholate was added to a final concentration of 2 mg/ml. After 10 min on ice, the sample was lysed by five cycles of sonication in 15-s bursts. The lysate was treated with DNase I (100 U/ml) for 30 min at 30 °C and centrifuged at 10,000*g* for 10 min.

The supernatant containing the VP1 protein was subjected to 20% sucrose cushion centrifugation at 100,000*g* for 3 h at 4 °C. The pellet was resuspended with reassociation buffer and purified by CsCl gradient centrifugation. The peak fraction of VP1 (density 1.29 g/ml) was then collected and dialyzed against the reassociation buffer. The morphology of VLP, which has a diameter of 45 nm, was confirmed by electron microscopy. VLPs were quantified by HA assay, as described previously [12].

Preparation of cell membrane fraction

IMR-32 cells were harvested, washed with PBS, and centrifuged for 3 min at 1000*g*. The cells were suspended in 5 volumes of a solution containing 0.25 M sucrose and 20 mM Hepes (pH 7.5), and disrupted with a glass Dounce homogenizer. The nuclei and unbroken cells were removed by centrifugation for 7 min at 1000*g*. The supernatant was transferred to a new centrifugation tube and pelleted at 105,000*g* for 1 h in a Hitachi P70AT rotor at 4 °C. The pellet was resuspended with 3 ml of a buffer containing 2.1 M sucrose and 20 mM Hepes (pH 7.5), and purified by sucrose gradient centrifugation. The peak fraction of the membrane fraction was collected and centrifuged for 1 h at 105,000*g*. The pellet was resuspended with 1 ml of a buffer containing 20 mM Tris–HCl (pH 7.5), 400 mM NaCl, 1% Triton X-100, 5 mM EDTA, and 1 mM PMSF in the presence of protease inhibitors (1 μg/ml aprotinin, 1 μg/ml pepstatin, and 1 mM DTT) and incubated at 4 °C for 30 min. The protein concentration was quantified by Bio-Rad (Hercules, CA) assay using bovine serum albumin as a standard.

Production of monoclonal antibodies against IMR-32 cell-membrane protein

BALB/c mice were immunized five times with 100 μg IMR-32 cell membrane fraction, emulsified in a Freund's complete adjuvant (Sigma) for primary immunization and in a Freund's incomplete adjuvant (Sigma) for four further immunizations at 7-day intervals. Dot-blot analysis and enzyme-linked immunosorbent assay (ELISA) were performed to confirm the immunoreactivity of sera against the IMR-32 cell membrane fraction. The mice that showed recognition of IMR-32 cell membrane fraction were boosted with a final immunization, and 4 days later the spleen cells from immunized animals were fused to P3U1 myeloma cells to produce approximately 600 hybridoma-containing wells.

Development of the immunoscreening system

We developed an immunoscreening system to isolate a monoclonal antibody that recognizes the JCV receptor from antibodies raised against IMR-32 cell membranes (Fig. 1A). As it is difficult to obtain sufficient amount of native JCV, we used VLPs instead of the native virion for immunoscreening.

A 96-well microtiter plate (Nalgen Nunc International, Rochester, NY) was coated with purified IMR-32 membrane fraction (1 μg/well) in 100 mM sodium bicarbonate buffer (pH 9.5). As a negative control, the wells were coated with BSA or left uncoated. Non-specific binding was blocked with PBS (pH 7.4) containing 25% Block Ace and 0.05% NaN_3. Aliquots of 200 μl of supernatant from each hybridoma were loaded onto each membrane-coated well, and the microtiter plate was incubated overnight at 4 °C. After washing three times with PBS, a solution of purified VLPs (5000 HA) was added to each well, followed by incubation at 37 °C for 1 h. The unbound VLPs were washed out with PBS. The plates were then incubated with a 1:1000 dilution of anti-VP1 antibody in EC buffer (20 mM phosphate buffer, pH 7.0, containing 400 mM NaCl, 2 mM EDTA, 10% Block Ace, 0.2% BSA, 0.05% NaN_3, and 0.075% Chaps) at room temperature for 2 h. After washing with PBS, a 1:5000 dilution of peroxidase-conjugated goat anti-rabbit immunoglobulin (Bio Source International, Camarillo, CA) in C buffer (20 mM phosphate buffer, pH 7.0, containing 400 mM NaCl, 2 mM EDTA, 10% Block Ace, 0.2% BSA, and 0.1% thimerosal) was added, and the plates were incubated for 3 h at room temperature. After washing three times, 100 μl of TMB reagent (Pierce Chemical, Rockford, IL) was added and developed for 15 min before quenching with an equal volume of 1 M phosphate buffer. The absorbance was measured at 450 nm with a microplate reader (Bio-Rad, Laboratories, Hercules, CA). In this system, antibodies that recognize VLP binding protein will inhibit binding of VLP to the membrane-coated well, while antibodies that do not recognize VLP binding protein will permit binding of VLP to the well.

To confirm the specificity of VLP binding to the IMR-32-coated wells, we examined the binding kinetics. Initially, we determined how much VLP was appropriate for detection of bound VLPs to the membrane-coated wells. The amounts of VLPs bound to the wells increased in a dose-dependent manner from 500 to 1×10^4 HAU, and reached saturation at a concentration of 1×10^5 HAU in both 0.5 and

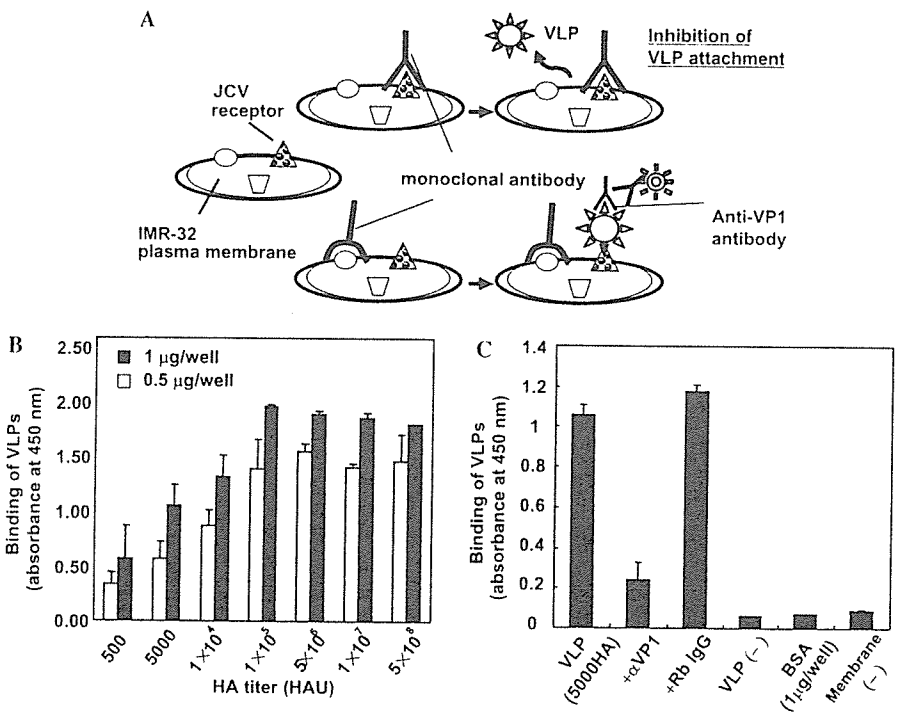

Fig. 1. Development of the immunoscreening system. (A) Strategy of the immunoscreening system using a blocking antibody against JCV infection. BALB/c mice are immunized with the membrane fraction from the human neuroblastoma cell line, IMR-32 cells. The wells of a 96-well plate are coated with the membrane fraction of IMR-32 cells, and then incubated with monoclonal antibodies derived from immunized mice before addition of VLPs. The amount of bound VLPs to the IMR-32 membrane fraction coated onto the wells is quantified with anti-VP1 antibody, followed by incubation with peroxidase-conjugated goat anti-rabbit immunoglobulins and TMB reagent. Absorbance was measured at 450 nm with a microplate reader. (B) The kinetics of binding of VLPs to IMR-32 membrane fractions. The amount of bound VLPs to the membrane fraction increased in a dose-dependent manner and peaked in the presence of 1×10^5 HAU VLPs. (C) Specificity of binding of VLPs to membrane-coated wells. The binding of VLPs was significantly inhibited in the presence of anti-VP1 antibody that recognizes JCV viral capsid protein, VP1, but was not affected in the presence of the isotype control rabbit normal IgG (Rb IgG). Negative controls, including VLP (−), BSA, and membrane (−), did not bind to the wells. The bars represent the standard deviation of the mean of at least three independent experiments performed in duplicate.

1 μg IMR-32 membrane protein-coated wells (Fig. 1B). In addition, a relatively low level of non-specific binding was recognized as compared with the negative control, and VLP binding was inhibited significantly in the presence of anti-VP1 antibody with application of 5000 HAU VLPs (Fig. 1C). Thus, it was demonstrated that VLPs bound to IMR-32 membranes in a specific manner in this immunoscreening system.

After immunoscreening of more than 600 clones, one clone, designated as "24D2," was identified as one of the antibodies showing the greatest inhibitory effect. The subtype of 24D2 was shown to be IgM using a monoclonal antibody isotype detection kit (Amersham–Pharmacia Biotech, Piscataway, NJ). The hybridoma cells were recloned to confirm the production of a monospecific antibody and cultured in a CELLine culture system (BD Biosciences, San Jose, CA) to obtain a large amount of the antibody. The concentration of the resulting supernatant was measured by semi-quantitative immunoblotting assay using mouse immunoglobulin as a standard. The antibody was separated by SDS–PAGE on a 10% gel. After blocking with 5% skim milk/PBST for 30 min, the anti-mouse immunoglobulins were diluted 1:5000 in PBST. Immunoreactive bands were detected by ECL (Amersham–Pharmacia Biotech) and analyzed with LAS-1000 Plus image analyzer (Fuji Film, Tokyo, Japan). The concentration of 24D2 was determined as the intensity relative to that of the control antibody.

Inhibition of VLP binding to IMR-32 cells by 24D2

For conjugation of purified VLPs with fluorescein isothiocyanate (FITC), aliquots of 2 mg of purified VLPs were dissolved in 0.1 M carbonate–bicarbonate buffer (pH 9.0), mixed with 156 μg FITC (Sigma), and incubated at room temperature for 2 h. To eliminate unlabeled FITC, the samples were centrifuged at 100,000*g* for 1 h at 4 °C. The pellet was dissolved in PBS, and centrifuged at 10,000*g* overnight, and the pellet was resuspended in PBS.

Before the experiment, IMR-32 cells (2×10^4) were plated onto 8-microwell tissue culture chambers (Nalgen Nunc International) and cultured in DMEM containing 10% FBS. The cells were pre-incubated in the absence or presence of either 24D2 (50 μg/ml) or isotype control monoclonal antibody for 1 h at 37 °C. Subsequently, FITC-VLPs (1×10^5 HAU) diluted 1:10 with DMEM were added to each chamber for 1 h at 4 °C. Unbound FITC-VLPs were removed by washing with PBS, and incubated for 15 min at 37 °C, following observation with a laser scanning confocal microscope (Olympus, Tokyo, Japan).

Inhibition of JCV infection by 24D2

IMR-32 cells (5×10^4) were preincubated in the absence or presence of either 24D2 (300 μg/ml) or the isotype control monoclonal antibody for 1 h at 37 °C. The cells were then incubated with 512 HAU JCV in fresh medium with 2% FBS for 1 h at 37 °C. After washing twice with fresh medium, the cells were incubated at 37 °C for 4 days with DMEM supplemented with 2% FBS. The monolayer culture in each well was washed with PBS and lysed in 1% Triton X-100/TBS containing 2 μg/ml aprotinin. The cell lysates were centrifuged at 4 °C for 10 min at 15,000 rpm, and the supernatants were separated by SDS–PAGE on 12% gels. After transferring the separated proteins onto a PVDF membrane, the membrane was immersed in 5% skim milk/TBS-T (20 mM Tris–HCl, pH 7.5, 150 mM NaCl, and 0.1% Tween 20) for 30 min, and subsequently incubated with either anti-agnoprotein antibody or anti-T-antigen antibody diluted 1:1000 with TBS-T for 1 h. After washing twice with TBS-T, the membrane was incubated with HRP-conjugated $F(ab')_2$ goat anti-rabbit or HRP-conjugated $F(ab')_2$ goat anti-mouse immunoglobulins diluted 1:5000 in TBS-T for 1 h. Immunoreactive bands were detected using the ECL reagent (Amersham–Pharmacia Biotech) and analyzed using an LAS-1000 plus image analyzer. Expression of viral proteins in the cells is represented as intensity relative to that of the control sample without treatment with 24D2 or isotype control antibody. The data are presented as mean values ± SD of three independent experiments.

Analysis of the molecule recognized by 24D2

Immunoblotting. Immunoblotting was performed as described above with the following modifications. The purified IMR-32 membrane fractions were separated by SDS–PAGE on 10% gels, transferred onto PVDF membranes, and immunoblotted with the 24D2 antibody. Immunoreactive bands were analyzed as described above.

Immunocytochemistry. IMR-32 cells grown on 8-microwell chambers were fixed with methanol at −80 °C for 2 min and rehydrated in PBS for 5 min at room temperature. After incubation with blocking solution (PBS containing 3% BSA), cells were incubated with 24D2 antibody diluted 1:60 in blocking solution for 2 h. After washing three times with PBS, the cells were incubated with Alexa Fluor 488-conjugated goat anti-mouse IgM antibody (Molecular Probes, Eugene, OR) diluted 1:500 for 1 h, and observed using a laser scanning confocal microscope (Olympus).

Immunohistochemistry. Normal human brain tissue obtained at autopsy was sectioned at a thickness of 10 μm with a Cryo 2000 cryostat (Sankyo, Tokyo, Japan) and fixed in acetone at 4 °C for 10 min. The sections were rinsed in PBS, blocked in 0.3% H_2O_2 methanol for 15 min, and incubated with 24D2 at 4 °C overnight. After incubation with biotinylated second antibody, immunoreactive products were visualized with 3,3′-diaminobenzidine. For double immunostaining of human brain tissue, the sections were rinsed twice in PBS, preincubated in PBS containing 3% BSA for 60 min, and incubated with anti-glial fibrillary acidic protein (GFAP, 1:5 dilution), anti-carbonic anhydrase-II (CA2, 1:1,000 dilution), or anti-synaptophysin (1:100 dilution) together with 24D2 (1:5) overnight. The sections were incubated with the appropriate secondary antibodies, including Alexa Fluor 488-conjugated goat anti-rabbit IgG, biotinylated anti-sheep IgG, Alexa Fluor 488-conjugated streptavidin, Alexa Fluor 488-conjugated goat anti-mouse IgG, or Alexa Fluor 594-conjugated goat anti-mouse IgM (Molecular Probes). After rinsing with PBS for 30 min, the sections were observed by laser scanning confocal microscopy.

Results

Isolation of monoclonal antibody (24D2) which inhibits attachment of JCV

Among more than 600 clones of monoclonal antibodies against the cell membrane fraction of JCV-permissive human neuroblastoma cell line IMR-32 cells, one hybridoma clone was isolated using the immunoscreening system and was designated as "24D2" (Fig. 1A). 24D2 significantly inhibited the binding of VLPs (Fig. 2A) as well as JCV (Fig. 2B) to cell membrane fractions on the immunoplates, whereas an isotype control antibody (mouse IgM) showed no inhibitory effect (Figs. 2A and B).

The 24D2 inhibits attachment and entry of FITC-labeled VLPs into IMR-32 cells

To evaluate the inhibitory effects on attachment and entry of VLPs, which have functions in cellular attachment and entry, similar to native JCV infection

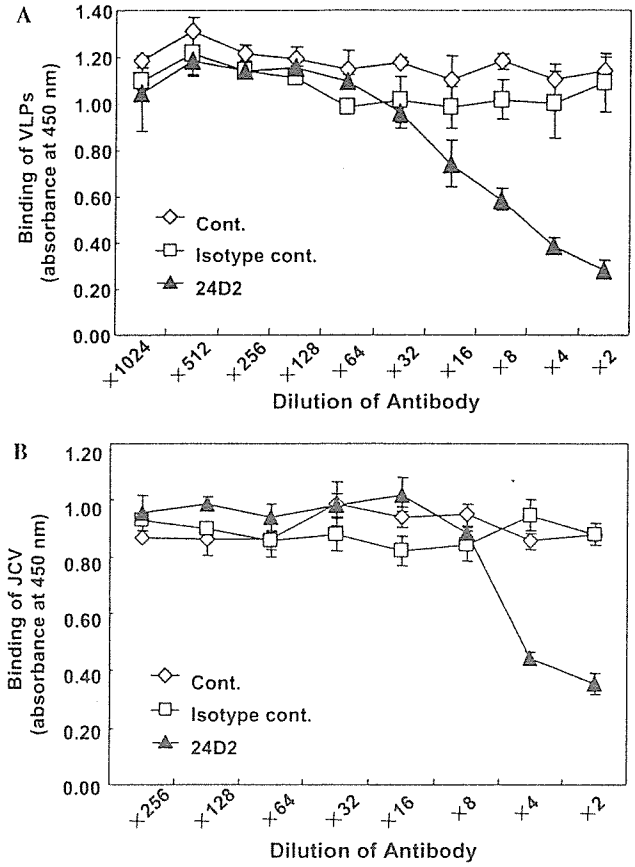

Fig. 2. Inhibition of the binding of both VLPs and JCV to IMR-32 membrane fractions on the immunoplate system by 24D2. (A,B) Inhibition of JCV and VLP binding by 24D2. IMR-32 membrane fractions were coated onto each well of the immunoplates, which were preincubated with serial dilutions of 24D2 (▲), mouse IgM (isotype control antibody, □), or without antibody (◇), and then incubated with 5000 HAU of VLPs (A) or JCV (B). Binding of VLPs or JCV was detected with anti-VP1 antibody and presented as the absorbance value. The bars represent the standard deviation of the mean of at least three independent experiments performed in duplicate.

[2,6] into IMR-32 cells, the cells were pretreated in the presence of either 24D2 or the isotype control monoclonal antibody, and incubated with FITC-labeled VLPs. 24D2 completely inhibited cellular attachment and entry of FITC-VLPs in IMR-32 cells, while the isotype control antibody had no effect on attachment or entry (Fig. 3).

Inhibition of JCV infection to IMR-32 cells by 24D2

To determine the blocking activity of 24D2 against JCV infection, IMR-32 cells were incubated with 24D2 before JCV inoculation. Four days after inoculation, expression of the viral proteins, including early and late viral proteins, T-antigen, and agnoprotein, was examined by immunoblotting. Treatment with 24D2 markedly inhibited expression of both T-antigen and agnoprotein in JCV-infected cells (Figs. 4A and B). The inhibitory effect of 24D2 against JCV infection was dose-dependent (Fig. 4C). Thus, we demonstrated that 24D2 possessed inhibition activity against JCV infection, suggesting that the molecule recognized by 24D2 plays a role as a cellular receptor for JCV.

Characterization of the molecule recognized by 24D2

We further characterized the molecule recognized by 24D2 by immunoblotting. 24D2 clearly recognized a single band with a molecular weight of around 60 kDa in membrane fractions from IMR-32 cells (Fig. 5A). Immunoblotting was also performed using various cell lines, including, HEK-293, HeLa, COS7, and SVG-A. In HEK293 cells, 24D2 recognized a single band with the same molecular weight as that of IMR-32 cells. However, in HeLa, COS7, and SVG-A cells, positive signals were observed around 30 kDa instead of 60 kDa (Fig. 5B).

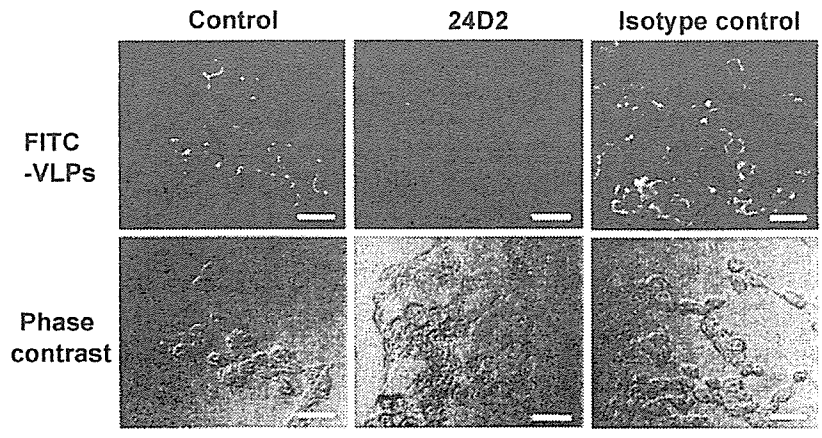

Fig. 3. Inhibitory effect of 24D2 on attachment and entry of FITC-labeled VLPs (FITC-VLPs) into IMR-32cells. After 1-h incubation with either 24D2 or the isotype control antibody, IMR-32 cells were incubated with FITC-VLPs. The immunofluorescence signal of FITC-VLPs was observed by confocal microscopy. No FITC signal was observed in cells treated with 24D2. Bars, 20 μm.

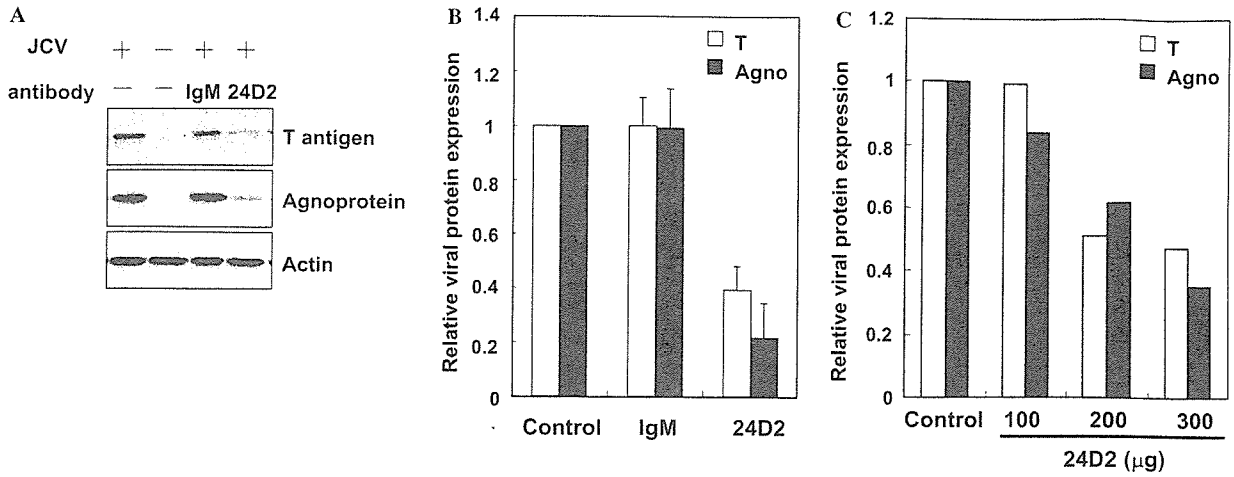

Fig. 4. Inhibition of JCV infection by treatment with 24D2. IMR-32 cells pretreated in the absence or presence of 24D2 or the isotype control antibody (IgM) were inoculated with 512 HAU of JCV for 1 h. Four days after inoculation, the cells were harvested and analyzed with immunoblotting using specific antibodies for JCV proteins (large T-antigen and agnoprotein). (A) Representative immunoblotting data with antibodies for large T-antigen and agnoprotein. Anti-actin antibody was used as a loading control. (B) Expression levels of viral proteins in IMR-32 cells treated with 24D2 or the isotype control antibody (IgM) relative to non-treated IMR-32 cells (control) at 4 days after inoculation of JCV. The bars represent mean values ± SD of at least three independent experiments. (C) The dose-dependent inhibition of JCV infection by 24D2. IMR-32 cells were incubated with different concentrations of 24D2 and incubated with 512 HAU JCV. JCV T-antigen and agnoprotein expression in IMR-32 cells was analyzed by immunoblotting 4 days after inoculation. The data are presented as amounts of viral protein expression relative to that of control infection. The assays were performed at least twice independently.

Next, we investigated the subcellular localization of positive signals with 24D2 in IMR-32 and HEK-293 cells by immunocytochemistry. The immunopositive signals for 24D2 were detected mainly on the cell surface and in the intracytoplasmic compartment (Fig. 5C). We performed the immunocytochemical examination using HeLa, COS, and SVG cells. In these cells, the immunopositive signals against 24D2 were also recognized in the cell surface and in the cytoplasm (data not shown).

The molecule recognized by 24D2 is localized mainly in glial cells in the human brain

Recently, it has been reported that JCV receptor-type α2–6-linked sialic acid was localized in oligodendrocytes and astrocytes but not in cortical neurons [13]. Although the viral genome was detected in various organs, such as the kidney, lymphoid tissue, lung, liver, and intestinal tract, the major target cells of JCV infection in the CNS are glial cells, such as oligodendrocytes and astrocytes [14,15]. Therefore, we investigated the subcellular localization of the molecule recognized by 24D2 in the human brain. Positive signals for 24D2 were distributed in the glial cells of the cerebrum and cerebellum (Fig. 6A). To confirm the cellular distribution of the immunopositive signals, we performed double immunofluorescence staining using 24D2 and cell-specific markers, such as CA2, as a marker of oligodendrocytes [16–19], GFAP, a marker of astrocytes, and synaptophysin, a neuronal marker (g–i) (Fig. 6B). The immunopositive signals of 24D2 were colocalized with GFAP and CA2 (Figs. 6Ba–f). However, 24D2 failed to react with synaptophysin-positive neurons (Fig. 6Bg–i). These results indicated that the molecule recognized by 24D2 is distributed mainly in glial cells in the human brain.

Discussion

Virus attachment to cell-surface molecules is an initial event in the process of virus infection. Many viruses utilize various receptors for attachment and entry into cells. The polyomavirus, simian vacuolating virus 40 (SV 40), binds to the MHC class I molecule at the cell surface [20], but the MHC molecule is not internalized into the cells together with SV 40 [21]. The ganglioside GM1 also binds to SV 40, and is mediated to transport the virus from the plasma membrane to the endoplasmic reticulum (ER), and a role of GM1 as a functional receptor has been suggested [22]. The mouse polyomavirus (PyV) is also known to bind to the sialic acid of an as yet unidentified receptor [23]. Efforts to identify the receptor by screening for monoclonal antibodies that can protect cells from infection have been unsuccessful [24]. It has been reported that an antibody to α4β1 integrin partially inhibits PyV infection [8]. Therefore, the integrin has been suggested to act as an entry receptor in the early stages of PyV infection in fibroblasts, and PyV utilizes gangliosides as carriers from the plasma membrane to the ER [22]. Interestingly, SV40 and PyV have been shown to use clathrin-independent and caveolin-

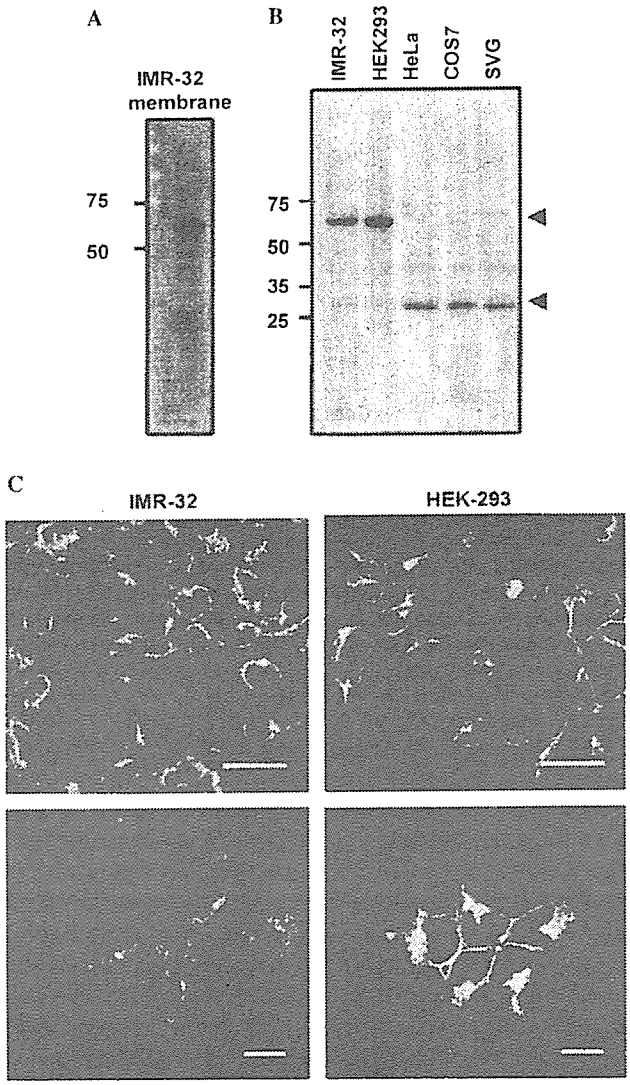

Fig. 5. Characterization of the molecule recognized by 24D2. (A) Immunoblotting analysis with membrane extracts derived from IMR-32 cells. Aliquots of 20 μg of the detergent-solubilized IMR-32 membrane fraction were loaded and immunoblotted with 24D2 at a dilution of 1:60. (B) Immunoblotting analysis with various cell lysates. The membrane fractions were prepared from IMR-32, HEK293, COS7, HeLa, and SVG-A cells. Molecular size markers are indicated on the left of the column. (C) Subcellular localization of the molecule recognized by 24D2 in IMR-32 and HEK-293 cells. Methanol-fixed cells were incubated with 24D2 at a dilution of 1:60, following Alexa Fluor 488-conjugated goat anti-mouse IgM. The immunofluorescence signal is represented as a green color. The lower panels show higher magnifications of the upper panels. Bars, 20 μm (upper panels) and 10 μm (lower panels).

dependent mechanisms to infect cells, respectively [25–27]. In contrast, JCV enters host cells by receptor-mediated clathrin-dependent endocytosis [28]. Furthermore, it has been reported that JCV does not share receptor specificity with SV 40 on human glial cells, because anti-class I antibodies failed to inhibit JCV infection [6].

It has been reported that a sialic acid-containing glycoprotein is one of the receptors of the human polyomavirus JCV in human glial cells, as neuraminidase treatment suppressed JCV attachment to the cells and subsequent infection [6].

In the present study, we have shown that the monoclonal antibody 24D2 inhibits JCV infection in IMR-32 cells. Although the major targets of JCV infection in the central nervous system are the glial cells, the viral genome was detected in various organs, such as the kidney, lymphoid tissue, lung, liver, and gastrointestinal tract [29–31], and JCV can enter a wide variety of cell types [5]. The 60-kDa molecule recognized by 24D2 was detected not only in IMR-32 cells, but also in other cell lines, including the human kidney cell line, HEK293. In addition, 24D2 showed inhibition of cellular attachment and entry of FITC-VLP to HEK293 cells (data not shown). These results suggest that the molecule recognized by 24D2 also acts as a receptor in IMR-32 and HEK293 cells. As 24D2 failed to completely inhibit infection, additional molecules might participate in JCV attachment and infection.

It is interesting to note that JCV has been suggested to persistently infect the kidney, because JCV genome was detected in the urine and the renal tissue of healthy individuals [32,33]. 24D2 also recognized a molecule of 30 kDa in the membrane fractions of HeLa, COS7, and SVG-A cells. This smaller molecule might be an isotype or a proteolytic product of the larger molecule. It has been reported that a monoclonal antibody against the hyaluronan receptor recognized two distinct receptors in the cell membranes of rat liver sinusoidal endothelial cells, which were identified previously as hyaluronan-binding proteins of 175 and 300 kDa [34,35]. After reduction of disulfide bonds, the 175-kDa hyaluronan receptor was shown to be a single protein, whereas the 300-kDa molecule consisted of three subunits, i.e., α (269 kDa), β (230 kDa), and γ subunits (97 kDa) [35], and it has been reported that the 175-kDa receptor was derived from the 300-kDa receptor by proteolytic processing [36]. Similar to the hyaluronan receptors, the molecules of 30 and 60 kDa recognized by 24D2 might be isoreceptors for the same ligand or products derived from a larger receptor complex. It has been reported that the receptor with 30-kDa molecular weight for human coronavirus OC43 was isolated from the newborn mouse brain membrane fractions [37]. A 30-kDa molecule detected in HeLa, COS7, and SVG cells might be similar to a coronavirus OC43 receptor.

We also examined the localization of the putative receptor molecule in the human brain, because JCV infects mainly glial cells in the central nervous system. Positive immunoreactivity for 24D2 was colocalized with CA2-positive oligodendrocytes and GFAP-positive astrocytes, but failed to colocalize with synaptophysin-positive neurons. These findings indicated that the putative receptor molecule for JCV was localized mainly in the glial cells of the human brain. In the present study,

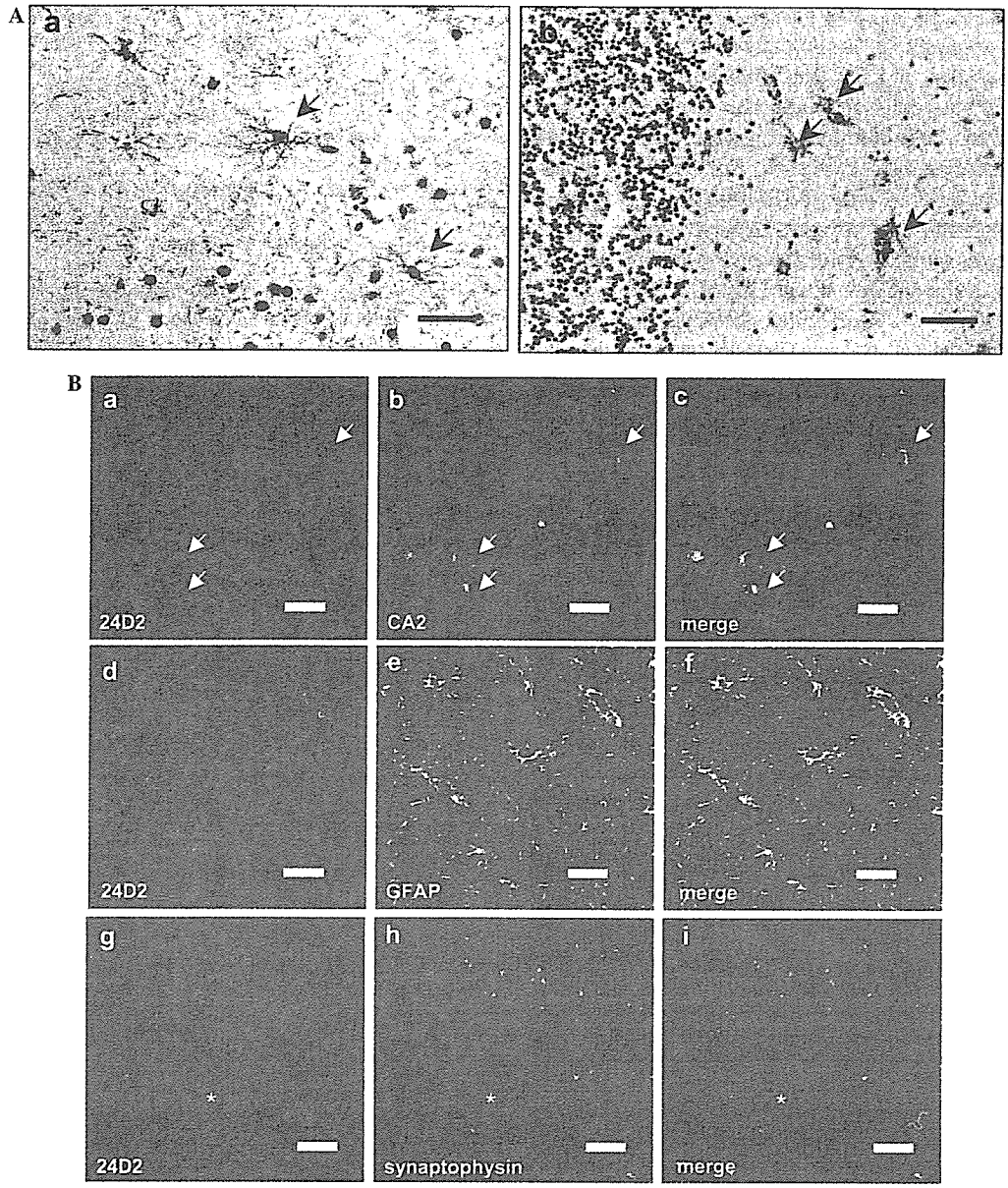

Fig. 6. Subcellular localization of the molecule recognized by 24D2 in the human brain. (A) Immunoreactivity with 24D2 in the cerebrum (a) and the cerebellum (b). Arrows indicate the immunopositive cells (a,b) in the white matter. Scale bars, 50 μm. (B) Double immunostaining using 24D2 and anti-CA2 antibody (a–c), anti-GFAP antibody (d–f), or anti-synaptophysin antibody (g–i) in the cerebrum. The merged images show that the molecule recognized by 24D2 (red color) was colocalized with CA2 and GFAP (green color). However, colocalization was not detected between 24D2 and anti-synaptophysin signals. Arrows indicate the 24D2- and CA2-double positive cells (a–c). Asterisks indicate white matter (g–i). Scale bars, 20 μm.

the neuroblastoma cell line, IMR-32, was used as the immunogen for the monoclonal antibody because these cells are highly susceptible to JCV infection [38]. Furthermore, immunization of IMR-32 cell has been shown to produce an antibody that specifically recognizes a molecule in oligodendrocytes [39]. Thus, it was suggested that IMR-32 cells possess molecules in common with brain glial cells. In Fig. 6Aa and b, the immunopositive signals against 24D2 were less than those of Fig. 6Ba, d, and g. We suppose that the difference of oligodendrocyte 24D2 immunostaining patterns among Fig. 6A and B might be due to the applied immunostaining systems. In Fig. 6A, we applied the biotinylated antibody as a second antibody, and the sections were observed with light microscopy. Meanwhile, in Fig. 6B, we observed the sections labeled with Alexa Fluor 488-conjugated second antibodies with fluorescent microscopy.

In summary, we have isolated a monoclonal antibody against the receptor molecule for JCV. By a newly established immunoscreening system, we isolated a monoclonal antibody (24D2) that inhibits cellular attachment

and infection of JCV. We also showed that the antibody specifically recognizes a membrane molecule with a molecular weight of 60 kDa, and positive signals were observed in the glial cells of the human brain. These results suggest that the molecule recognized by 24D2 acts as a JCV receptor in JCV infection. Further studies are required to characterize and determine the functional role of the molecule. A greater understanding of the molecular characteristics of the receptor molecule is necessary for the design of novel anti-JCV agents. Experiments to identify the molecules detected by 24D2 using a λ phage library are currently in progress in our laboratory.

Note added in proof

Recently, it has been reported that the antagonists and antibodies against the 5HT2 serotonergic receptors blocked JCV infection in SVG-A cells [40], suggesting that serotonin receptors act as one of the JCV receptors.

Acknowledgments

We thank Ms. M. Sato for expert technical assistance, Dr. K. Iwabuchi for the generous gift of the mouse myeloma cells, and Drs. S. Semba, R. Komagome, Y. Okada, and S. Endo for their valuable suggestions. We also thank T. Suzuki for critical help with computer graphics. This work was supported in part by grants from the Ministry of Education, Science, Technology, Sports and Culture of Japan, the Ministry of Health, Labor, and Welfare of Japan, and the Japan Human Science Foundation.

References

[1] E.O. Major, K. Amemiya, C.S. Tornatore, S.A. Houff, J.R. Berger, Pathogenesis and molecular biology of progressive multifocal leukoencephalopathy, the JC virus-induced demyelinating disease of the human brain, Clin. Microbiol. Rev 5 (1992) 49–73.

[2] Q. Qu, H. Sawa, T. Suzuki, S. Semba, C. Henmi, Y. Okada, M. Tsuda, S. Tanaka, W.J. Atwood, K. Nagashima, Nuclear entry mechanism of the human polyomavirus JC virus-like particle: role of importins and the nuclear pore complex, J. Biol. Chem. 279 (2004) 27735–27742.

[3] C. Goldmann, H. Petry, S. Frye, O. Ast, S. Ebitsch, K.D. Jentsch, F.J. Kaup, F. Weber, C. Trebst, T. Nisslein, G. Hunsmann, T. Weber, W. Luke, Molecular cloning and expression of major structural protein VP1 of the human polyomavirus JC virus: formation of virus-like particles useful for immunological and therapeutic studies, J. Virol. 73 (1999) 4465–4469.

[4] R. Komagome, H. Sawa, T. Suzuki, Y. Suzuki, S. Tanaka, W.J. Atwood, K. Nagashima, Oligosaccharides as receptors for JC virus, J. Virol. 76 (2002) 12992–13000.

[5] S. Suzuki, H. Sawa, R. Komagome, Y. Orba, M. Yamada, Y. Okada, Y. Ishida, H. Nishihara, S. Tanaka, K. Nagashima, Broad distribution of the JC virus receptor contrasts with a marked cellular restriction of virus replication, Virology 286 (2001) 100–112.

[6] C.K. Liu, G. Wei, W.J. Atwood, Infection of glial cells by the human polyomavirus JC is mediated by an N-linked glycoprotein containing terminal alpha (2–6)-linked sialic acids, J. Virol. 72 (1998) 4643–4649.

[7] W. Querbes, A. Benmerah, D. Tosoni, P.P. Di Fiore, W.J. Atwood, A JC virus-induced signal is required for infection of glial cells by a clathrin- and eps15-dependent pathway, J. Virol. 78 (2004) 250–256.

[8] M. Caruso, L. Belloni, O. Sthandier, P. Amati, M.I. Garcia, Alpha4beta1 integrin acts as a cell receptor for murine polyomavirus at the postattachment level, J. Virol. 77 (2003) 3913–3921.

[9] E.O. Major, A.E. Miller, P. Mourrain, R.G. Traub, E. de Widt, J. Sever, Establishment of a line of human fetal glial cells that supports JC virus multiplication, Proc. Natl. Acad. Sci. USA 82 (1985) 1257–1261.

[10] S. Endo, Y. Okada, Y. Orba, H. Nishihara, S. Tanaka, K. Nagashima, H. Sawa, JC virus agnoprotein colocalizes with tubulin, J. Neurovirol. 9 (Suppl. 1) (2003) 10–14.

[11] Y. Okada, H. Sawa, S. Tanaka, A. Takada, S. Suzuki, H. Hasegawa, T. Umemura, J. Fujisawa, Y. Tanaka, W.W. Hall, K. Nagashima, Transcriptional activation of JC virus by human T-lymphotropic virus type I Tax protein in human neuronal cell lines, J. Biol. Chem. 275 (2000) 17016–17023.

[12] T. Suzuki, A. Portner, R.A. Scroggs, M. Uchikawa, N. Koyama, K. Matsuo, Y. Suzuki, T. Takimoto, Receptor specificities of human respiroviruses, J. Virol. 75 (2001) 4604–4613.

[13] S. Eash, R. Tavares, E.G. Stopa, S.H. Robbins, L. Brossay, W.J. Atwood, Differential distribution of the JC virus receptor-type sialic acid in normal human tissues, Am. J. Pathol. 164 (2004) 419–428.

[14] Y. Okada, H. Sawa, S. Endo, Y. Orba, T. Umemura, H. Nishihara, A.C. Stan, S. Tanaka, H. Takahashi, K. Nagashima, Expression of JC virus agnoprotein in progressive multifocal leukoencephalopathy brain, Acta Neuropathol. (Berl.) 104 (2002) 130–136.

[15] G.L. Stoner, H.T. Agostini, C.F. Ryschkewitsch, M. Mazlo, F. Gullotta, W. Wamukota, S. Lucas, Detection of JC virus in two African cases of progressive multifocal leukoencephalopathy including identification of JCV type 3 in a Gambian AIDS patient, J. Med. Microbiol. 47 (1998) 733–742.

[16] G.C. DeLuca, Z. Nagy, M.M. Esiri, P. Davey, Evidence for a role for apoptosis in central pontine myelinolysis, Acta Neuropathol. (Berl.) 103 (2002) 590–598.

[17] M.S. Ghandour, O.K. Langley, G. Vincendon, G. Gombos, D. Filippi, N. Limozin, D. Dalmasso, G. Laurent, Immunochemical and immunohistochemical study of carbonic anhydrase II in adult rat cerebellum: a marker for oligodendrocytes, Neuroscience 5 (1980) 559–571.

[18] M.S. Ghandour, A.K. Parkkila, S. Parkkila, A. Waheed, W.S. Sly, Mitochondrial carbonic anhydrase in the nervous system: expression in neuronal and glial cells, J. Neurochem. 75 (2000) 2212–2220.

[19] R.P. Skoff, M.S. Ghandour, Oligodendrocytes in female carriers of the jimpy gene make more myelin than normal oligodendrocytes, J. Comp. Neurol. 355 (1995) 124–133.

[20] W.C. Breau, W.J. Atwood, L.C. Norkin, Class I major histocompatibility proteins are an essential component of the simian virus 40 receptor, J. Virol. 66 (1992) 2037–2045.

[21] H.A. Anderson, Y. Chen, L.C. Norkin, MHC class I molecules are enriched in caveolae but do not enter with simian virus 40, J. Gen. Virol. 79 (1998) 1469–1477.

[22] B. Tsai, J.M. Gilbert, T. Stehle, W. Lencer, T.L. Benjamin, T.A. Rapoport, Gangliosides are receptors for murine polyoma virus and SV40, EMBO J. 22 (2003) 4346–4355.

[23] H. Fried, L.D. Cahan, J.C. Paulson, Polyoma virus recognizes specific sialyligosaccharide receptors on host cells, Virology 109 (1981) 188–192.
[24] P.H. Bauer, C. Cui, R. Liu, T. Stehle, S.C. Harrison, J.A. DeCaprio, T.L. Benjamin, Discrimination between sialic acid-containing receptors and pseudoreceptors regulates polyomavirus spread in the mouse, J. Virol. 73 (1999) 5826–5832.
[25] L. Pelkmans, J. Kartenbeck, A. Helenius, Caveolar endocytosis of simian virus 40 reveals a new two-step vesicular-transport pathway to the ER, Nat. Cell Biol. 3 (2001) 473–483.
[26] Z. Richterova, D. Liebl, M. Horak, Z. Palkova, J. Stokrova, P. Hozak, J. Korb, J. Forstova, Caveolae are involved in the trafficking of mouse polyomavirus virions and artificial VP1 pseudocapsids toward cell nuclei, J. Virol. 75 (2001) 10880–10891.
[27] E. Stang, J. Kartenbeck, R.G. Parton, Major histocompatibility complex class I molecules mediate association of SV40 with caveolae, Mol. Biol. Cell 8 (1997) 47–57.
[28] M.T. Pho, A. Ashok, W.J. Atwood, JC virus enters human glial cells by clathrin-dependent receptor-mediated endocytosis, J. Virol. 74 (2000) 2288–2292.
[29] B.W. Grinnell, B.L. Padgett, D.L. Walker, Distribution of nonintegrated DNA from JC papovavirus in organs of patients with progressive multifocal leukoencephalopathy, J. Infect. Dis. 147 (1983) 669–675.
[30] J.T. Newman, R.J. Frisque, Detection of archetype and rearranged variants of JC virus in multiple tissues from a pediatric PML patient, J. Med. Virol. 52 (1997) 243–252.
[31] L. Ricciardiello, L. Laghi, P. Ramamirtham, C.L. Chang, D.K. Chang, A.E. Randolph, C.R. Boland, JC virus DNA sequences are frequently present in the human upper and lower gastrointestinal tract, Gastroenterology 119 (2000) 1228–1235.
[32] T. Kitamura, C. Sugimoto, A. Kato, H. Ebihara, M. Suzuki, F. Taguchi, K. Kawabe, Y. Yogo, Persistent JC virus (JCV) infection is demonstrated by continuous shedding of the same JCV strains, J. Clin. Microbiol. 35 (1997) 1255–1257.
[33] T. Tominaga, Y. Yogo, T. Kitamura, Y. Aso, Persistence of archetypal JC virus DNA in normal renal tissue derived from tumor-bearing patients, Virology 186 (1992) 736–741.
[34] J.A. Weigel, R.C. Raymond, C. McGary, A. Singh, P.H. Weigel, A blocking antibody to the hyaluronan receptor for endocytosis (HARE) inhibits hyaluronan clearance by perfused liver, J. Biol. Chem. 278 (2003) 9808–9812.
[35] B. Zhou, J.A. Oka, A. Singh, P.H. Weigel, Purification and subunit characterization of the rat liver endocytic hyaluronan receptor, J. Biol. Chem. 274 (1999) 33831–33834.
[36] B. Zhou, J.A. Weigel, A. Saxena, P.H. Weigel, Molecular cloning and functional expression of the rat 175-kDa hyaluronan receptor for endocytosis, Mol. Biol. Cell 13 (2002) 2853–2868.
[37] A.R. Collins, Identification of 120 kD and 30 kD receptors for human coronavirus OC43 in cell membrane preparations from newborn mouse brain, Adv. Exp. Med. Biol. 380 (1995) 387–390.
[38] S. Nukuzuma, Y. Yogo, J. Guo, C. Nukuzuma, S. Itoh, T. Shinohara, K. Nagashima, Establishment and characterization of a carrier cell culture producing high titres of polyoma JC virus, J. Med. Virol. 47 (1995) 370–377.
[39] K. Yoshimura, F. Kametani, Y. Shimoda, K. Fujimaki, Y. Sakurai, K. Kitamura, H. Asou, M. Nomura, Antigens of monoclonal antibody NB3C4 are novel markers for oligodendrocytes, Neuroreport 12 (2001) 417–421.
[40] G.F. Elphick, W. Quebes, J.A. Jordan, G.V. Gee, S. Eash, K. Manley, A. Dugan, M. Stanifer, A. Bhatnagar, W.K. Kroeze, B.L. Roth, W.J. Atwood, The human polyomavirus, JCV, uses serotonin receptors to infect cells, Science 306 (2004) 1380–1383.

REVIEW ARTICLES

The Agnoprotein of Polyomaviruses: A Multifunctional Auxiliary Protein

KAMEL KHALILI,[1]* MARTYN K. WHITE,[1] HIROFUMI SAWA,[2,3] KAZUO NAGASHIMA,[2] AND MAHMUT SAFAK[1]

[1]*Center for Neurovirology and Cancer Biology, College of Science and Technology, Temple University, Philadelphia, Pennsylvania*

[2]*Laboratory of Molecular and Cellular Pathology, Hokkaido University School of Medicine, and CREST, JST, Sapporo, Japan*

[3]*21st Century COE Program for Zoonosis Control, Hokkaido University School of Medicine, and CREST, JST, Sapporo, Japan*

The late region of the three primate polyomaviruses (JCV, BKV, and SV40) encodes a small, highly basic protein known as agnoprotein. While much attention during the last two decades has focused on the transforming proteins encoded by the early region (small and large T-antigens), it has become increasingly evident that agnoprotein has a critical role in the regulation of viral gene expression and replication, and in the modulation of certain important host cell functions including cell cycle progression and DNA repair. The importance of agnoprotein is underscored by its expression during lytic infection of glial cells by JCV that occurs in progressive multifocal leukoencephalopathy (PML), and also in some JCV-associated human neural tumors particularly medulloblastoma. In this review, we will discuss the structure and function of agnoprotein in the viral life cycle during the course of lytic infection and the consequences of agnoprotein expression for the host cell. J. Cell. Physiol. 204: 1–7, 2005. © 2004 Wiley-Liss, Inc.

Many viruses encode minor gene products that are often small in size and serve an auxiliary function, i.e., they interact with cellular proteins or other viral proteins to facilitate the life cycle of the virus and in some cases the state of latency. Auxiliary proteins can have diverse effects on various stages of the viral infection cycle including replication, transcription, nuclear RNA export, translation, viral assembly, and release of viral particles from the cell. In this article, we focus our attention on the agnoprotein of polyomaviruses and discuss its role in the regulation of polyomavirus gene expression and replication and review recent discoveries on the impact of this protein on various host cell functions including cell-cycle regulation, DNA repair, and others.

Polyomaviruses are a family of small non-enveloped DNA viruses with icosahedral capsids containing small, circular, double-stranded DNA genomes. These viruses have been isolated from humans, monkeys, rodents, and birds. Two types of polyomaviral genome have been recognized (Cole, 1996). Mouse polyoma virus and other closely related rodent polyomaviruses have an early region that encodes three T-antigens (large-T, middle-T, and small-t) and a late region that encodes three capsid proteins VP1, VP2, and VP3. The primate polyomaviruses (SV40, JCV, and BKV) have an early region that encodes only two T-antigens (large-T and small-t) but contain an additional gene in the late region encoding a late auxiliary protein known as agnoprotein. It should also be noted that, in the case of JCV, three additional forms of T-antigen (T'_{135}, T'_{136}, and T'_{165}) have been identified that are generated by alternative splicing (Trowbridge and Frisque, 1995). The T' proteins interact differentially with proteins of the retinoblastoma family (Bollag et al., 2000), and may contribute to viral DNA replication (Prins and Frisque, 2001) and cell transformation (Frisque, 2001; Frisque et al., 2003).

In recent years, among the polyomaviruses, JCV has received special attention partly due to the AIDS epidemic. This virus which infects greater than 75% of human populations worldwide is an established etiological agent for the fatal demyelination disease, progressive multifocal leukoencephalopathy (PML). Once a rare disorder seen primarily in patients with an impaired immune system, PML has become more relevant clinically as nearly 5% of AIDS patients exhibit PML at the latter stages of their disease (Berger, 2003). In addition, results from molecular and histological techniques have provided compelling evidence for the association of JCV with various human neural tumors particularly medulloblastoma (Krynska et al., 1999; Del Valle et al., 2002b). Similar to other primate polyomaviruses, the JCV genome contains an open reading frame for an auxiliary protein, agnoprotein, in the viral late region which exhibits substantial homology with those from the well-studied SV40 polyomavirus and another human polyomavirus, BKV. In this short review, we visit all documented works on polyomavirus agnoprotein structure and function with respect to viral replication and host function. Particular attention will be paid to JCV agnoprotein and the early work on SV40 agnoprotein. The possibility of the existence of an auxiliary protein encoded in the viral early region is also discussed.

IDENTIFICATION OF AGNOPROTEIN

In the late 1970s, SV40 was among the first organisms for which entire genome sequence information became available. The sequence of the genome of SV40 virus (Fiers et al., 1978; Reddy et al., 1978) revealed the

Contract grant sponsor: NIH (to MS and KK).

*Correspondence to: Kamel Khalili, Center for Neurovirology and Cancer Biology, College of Science and Technology, Temple University, 1900 North 12th Street, 015-96, Room 203, Philadelphia, Pennsylvania 19122. E-mail: kamel.khalili@temple.edu

Received 6 October 2004; Accepted 12 October 2004

DOI: 10.1002/jcp.20266

presence of a small open reading frame in the proximal late region that was named agnogene since its function was unknown at the time (Dhar et al., 1977). The SV40 agnogene product was identified as a protein (agnoprotein) with a molecular weight of 7.9 kDa that is produced late in infection. It has a short half-life (2 h), is highly basic (pI = 10.6) and binds to both single and double-stranded DNA (Jay et al., 1981). Analysis of SV40-infected cells by CsCl density gradient centrifugation revealed that agnoprotein was associated with viral nucleoproteins but not with mature virions (Jackson and Chalkley, 1981). Comparison of the sequences of the genomes of the three primate polyomaviruses SV40, JC virus (JCV), and BK virus (BKV) indicated the presence of agnogenes encoding proteins of 62, 71, and 66 amino acids in length, respectively (Cole, 1996). It has also been shown that agnogene is expressed in the case of the human polyomavirus BKV (Rinaldo et al., 1998). BKV agnoprotein appears in the perinuclear area and cytoplasm late in the infectious cycle, is phosphorylated in vivo and coimmunoprecipitates with a subset of host cell proteins. Similarly, agnoprotein expression has been detected by Western blotting during the course of infection of glial cells by JCV (Okada et al., 2002; Safak et al., 2002; Endo et al., 2003; Radhakrishnan et al., 2003).

STRUCTURAL FEATURES OF AGNOPROTEIN

Figure 1A illustrates the structural organization of the genomes of the primate polyomaviruses showing the coding regions for the viral early regulatory proteins (large T-antigen and small t-antigen), and the late structural proteins (VP1, VP2, and VP3). The location of the agnogene in the 5′ proximal part of the late region is indicated. Figure 1B shows a comparison of the sequences of agnoprotein for JCV, BKV, and SV40. There is a high degree of sequence conservation between the polyomaviral agnoprotein for the region comprising the N-terminal and central domains, especially for JCV and BKV. The carboxy termini of agnoprotein show significant diversity in amino acid sequence. Of the 71 amino-acid residues in JCV agnoprotein, 41 are conserved in BKV agnoprotein and 30 of these are in the N-terminal 36 amino acids (Fig. 1B). The N-terminal amino acids 1–36 of JCV agnoprotein show 83% sequence identity with BKV agnoprotein, while amino

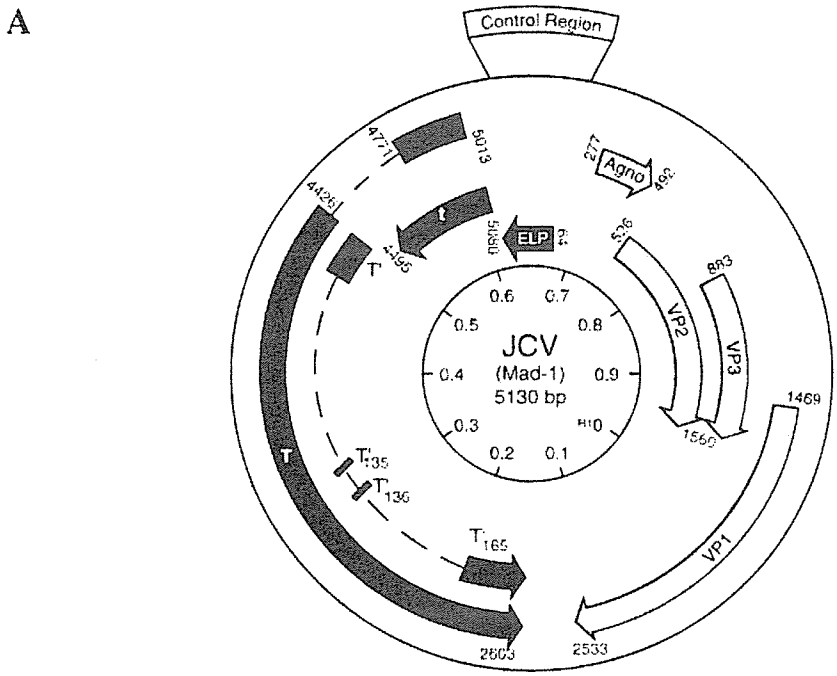

B

```
                10        20        30        40        50        60        70
JCV   MVLRQLSRKASVKVSKTWSGTKKRAQRILIFLLEFLLDFCTGEDSVDGKKRQRHSGLTEQTYSALPEPKAT
      |||||||:|||||:|||:|||||||||:||:||:::|| |. |||||:::
BKV   MVLRQLSRQASVKVGKTWTGTKKRAQRIFIFILELLLEFCRGEDSVDGKNKSTTALPAVKDSVKDS
      |||:|||:|||||  ::|: :|| |||:::|:||:|:|| |  :|||| ::
SV40  MVLRRLSRQASVKVRRSWTESKKTAQRLFVFVLELLLQFCEGEDTVDGKRKKPERLTEKPES
                10        20        30        40        50        60
```

Fig. 1. **A**: Schematic representation of the genomic organization of a primate polyomavirus. The early and late coding regions of the circular primate polyomavirus genome are shown and are separated by the non-coding regulatory region. Arrows indicate the direction of transcription. The numbering of the nucleotides is relative to the Mad-1 reference strain of JCV (GenBank # NC_001699). Agnoprotein and early leader protein (ELP) are found in the 5′ proximal regions of the late and early regions, respectively. Alternative splicing of the early region can also give rise to three variants of T-antigen (T'_{135}, T'_{136}, and T'_{165}). **B**: Comparison of the amino acid sequence of JCV agnoprotein to BKV and SV40 agnoproteins. The amino acid sequence of JCV agnoprotein (GenBank # NC_001699) was compared to the sequence of the agnoproteins of BKV (NC_001538) and SV40 (NC_001669). Sequence identity is indicated with a tilde (|). Conservative sequence changes are indicated with a colon (:). Amino acids that are identical in all three polyomaviruses are shown in bold face. Alignment was generated with the FASTA algorithm (Lipman and Pearson, 1985).

acids 37–50 show 73% identity and the C-terminal amino acids (51–71) show no significant homology at all. Interestingly, analysis of the predicted amino acid sequences of agnoprotein for 100 JCV isolates revealed that all but one of the sequence polymorphisms that were found in the study reside in this region (Cubitt et al., 2001). Also, a variant of JCV has been discovered in which these C-terminal 21 amino acids are deleted (Jobes et al., 1999). In contrast, the N-terminal region of agnoprotein is highly conserved; the six amino residues that vary between JCV and BKV in region 1–36 are all conservative changes (indicated by ":" in Fig. 1B). This likely indicates that this region is of strong functional importance. In the case of SV40, the N-terminal amino acids 1–36 show 61% sequence identity with JCV and of the 14 amino acid differences that occur in this region, 11 are conservative and 3 are not.

Analysis of the predicted hydrophilicity of agnoprotein (von Heijne, 1981) indicates that the N- and C-terminal domains are hydrophilic while the central portion of the protein is relatively hydrophobic (Fig. 2A). The predicted secondary structure (Garnier et al., 1978) suggests the presence of several potential helix-turn-helix domains and that the central domain may adopt an α-helical conformation (Fig. 2B). Agnoproteins are very basic proteins, e.g., JCV agnoprotein has a predicted isoelectric point of 10.1. They also contain potential sites for serine/threonine phosphorylation, e.g., JCV agnoprotein contains several serine and three threonines that reside within phosphorylation site motifs for known serine/threonine-specific protein kinases. It has been suggested that phosphorylation regulates the subcellular localization of JCV agnoprotein (Okada et al., 2001). In the case of BKV, metabolic labeling of BKV-infected cells with [^{32}P]-orthophosphate followed by agnoprotein immunoprecipitation has provided direct evidence for in vivo agnoprotein phosphorylation (Rinaldo et al., 1998). Investigation of the role of post-translational modifications in the regulation of agnoprotein function offers a potentially important area for future research.

EARLY STUDIES OF THE ROLE OF SV40 AGNOPROTEIN IN THE VIRAL LIFE CYCLE

Agnoprotein is encoded by the leader region of some species of SV40 late mRNA and accumulates in the perinuclear region of cells late in the infective cycle (Jay et al., 1981; Nomura et al., 1983). A minor but detectable fraction of agnoprotein was also found in the nucleus. Experiments comparing wild-type to agnoprotein-negative mutants of SV40 revealed that agnoprotein is involved in the perinuclear localization of VP1 (but not VP2 or VP3) during virion assembly and maturation (Carswell and Alwine, 1986; Resnick and Shenk, 1986). Agnoprotein-negative SV40 mutants are viable, but they produce infectious progeny more slowly than wild-type virus and are characterized by small plaque size (Mertz et al., 1983). During infection, these mutants are unaffected in progression from viral chromatin to previrions and contain similar levels of virion proteins to wild-type-infected cells but show defective virion maturation (Ng et al., 1985; Hou-Jong et al., 1987). Interestingly a series of second-site pseudorevertants of a partially defective VP1 mutant mapped to a serine codon near the beginning of the agnogene (Margolskee and Nathans, 1983). Similarly missense mutations in the *VP1* gene can compensate for defects caused by deletions in the viral agnogene (Barkan et al., 1987). Taken together, these data suggest that the SV40 agnoprotein interacts in a specific way with VP1 during the late stages of viral development to localize it within the cell and facilitate virion assembly and maturation.

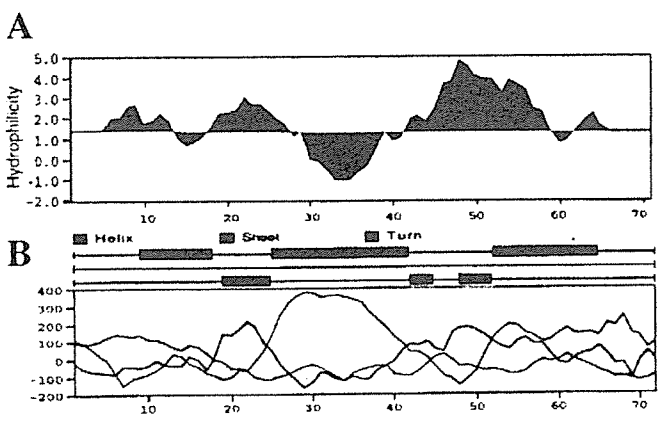

Fig. 2. Structural predictions for JCV agnoprotein. **A**: The chart shows the predicted hydrophilicity of regions of agnoprotein calculated by the method of von Heijne (1981) plotted against amino acid residue number (X-axis). **B**: The chart shows the Robson Garnier secondary structure prediction for agnoprotein (Garnier et al., 1978).

The effects of mutations in the SV40 agnogene on virion maturation are mediated by the *trans*-acting effect of agnoprotein. However, because the agnogene is located at the 5′-end of the late region and is present in the leader sequence of late mRNAs, agnogene mutations can also have *cis*-acting effects on the synthesis of late gene products. For example, an SV40 agnoprotein 12 bp deletion mutant has a potential secondary structure at the 5′-end of the leader RNA in which the start codon of agnoprotein is sequestered in a stem and shows reduced agnoprotein synthesis (Hay et al., 1984). Attenuation of late transcription and modulation of the secondary structure of the leader sequence of the late mRNA have been suggested as possible mechanisms for regulating late gene expression (Aloni and Hay, 1983; Hay and Aloni, 1985). This may serve to optimize the stoichiometry of the gene products of the late region during the course of infection with agnoprotein synthesis increasing towards the end of the infectious cycle. A 2 bp insertional mutant of agnogene has been described that has a far more deleterious effect on growth than deletion of the entire agnogene. Growth inhibition could be reversed by spontaneous second-site deletion mutations and may be due to an effect on the SV40 late mRNA precursor molecule (Nomura et al., 1986). There is also evidence that the relative positions of the AUG start codons for agnoprotein and viral capsid proteins relative to each other and the 5′-CAP site of the late mRNA can influence the rate of translation of the SV40 late proteins (Grass and Manley, 1987; Perez et al., 1987; Dabrowski and Alwine, 1988; Sedman et al., 1990).

In order to differentiate *cis*-acting from *trans*-acting effects of agnogene mutants, CV-1P cell lines have been constructed in which the SV40 agnogene is stably integrated and constitutively expressed (Carswell et al., 1986). Agnoprotein was located predominantly in the cytoplasmic and perinuclear region in these cells. Viruses that were agnoprotein-minus formed small plaques on normal CV-1P cells, but produced nearly wild-type-sized plaques on cells expressing a low level of agnoprotein. Conversely, cells expressing high levels of agnoprotein that were infected with agnoprotein-minus mutants formed plaques that were markedly smaller than the plaques formed by these viruses when they were grown on control cells. These results confirm that

the SV40 agnoprotein is a *trans*-effector of virus production and suggest that the nature of the effect of the agnoprotein on virus production may vary depending on its intracellular concentration.

Further insights into the role of agnoprotein in the life cycle of SV40 were gained by the analysis of C-terminal deletion mutants of T-antigen. These mutants are called host range mutants because they form plaques on BSC-1 and Vero but not on CV-1P monkey kidney cells (Stacy et al., 1989). These mutants demonstrate that the SV40 early protein T-antigen has a role in the late phase of the infective cycle. The level of late RNA is lower by a factor of 5–15 in CV-1P monkey cells infected with these mutants compared to cells infected with wild-type SV40. A comparable decrease occurs in the synthesis of VP1 and VP3 while the synthesis of SV40 agnoprotein decreases by a factor greater than 100 (Khalili et al., 1988). The ablation of synthesis of agnoprotein in mutant-infected CV-1 cells was due to the utilization of transcription start sites for late mRNA synthesis that lay downstream from the major wild-type cap site and the agnoprotein initiation codon. Thus the deletion of the carboxyl-terminal domain of T antigen affects both viral capsid protein synthesis and, through its action on agnoprotein, the assembly and maturation of virions (Stacy et al., 1989). Direct evidence for a defect in virion assembly and maturation in the C-terminal T-antigen mutants has been provided by sucrose density gradient analysis of virus-infected cell extracts (Spence and Pipas, 1994). Intercistronic complementation of these mutants could be achieved with mutants of SV40 that were defective in agnoprotein but produced wild-type T-antigen. This resulted in an increased synthesis of agnoprotein in the infected cells. Finally, it was found that CV-1 cells that constitutively express the SV40 agnoprotein were permissive for plaque formation by the T-antigen C-terminal host range mutants (Spence et al., 1990; Stacy et al., 1990).

STUDIES OF THE FUNCTION OF JCV AGNOPROTEIN

JCV is a human polyomavirus that is widespread throughout the human population and is clinically relevant for two reasons. Firstly, under conditions of immunosuppression, e.g., AIDS, the virus can replicate in the brain, destroying glial cells and causing the fatal demyelination disease PML. Secondly, JCV is associated with various human neural tumors particularly medulloblastoma (Krynska et al., 1999; Del Valle et al., 2002b). In this section, we will focus on molecular studies of JCV agnoprotein. Agnoprotein expression in clinical samples will be discussed later. In cells infected by JCV, the 8 kDa agnoprotein is produced late in the infectious cycle and is found mainly in the cytoplasm, especially in the perinuclear region, while a small amount may also be found in the nucleus (Okada et al., 2001; Safak et al., 2002). A similar localization was observed in cells transfected with a plasmid encoding agnoprotein (Darbinyan et al., 2002). When a JCV derivative containing portions of the SV40 regulatory region (Mad-1/SVEΔ) was used to infect SVG-A human fetal glial cells (which produce SV40 T-antigen but not SV40 agnoprotein), expression of JCV agnoprotein could be detected by Western blot within only 3 days post-infection (Safak et al., 2002).

Analysis of a point mutation at the initiation codon of agnoprotein translation indicated an essential role for agnoprotein in JCV gene expression. In neuroblastoma cells transfected with wild-type Mad-1 JCV DNA, mRNAs for T-antigen, agnoprotein and VP1 were detectable by RT-PCR. However, expression was not detected for the agnoprotein-negative mutant (Okada et al., 2001). Thus, unlike SV40, JCV agnoprotein has a critical role in viral DNA replication and transcription. Transfection studies of human glioblastoma cells with plasmids expressing agnoprotein have shown that it can negatively regulate JCV DNA replication and transcription from the JCV late promoter through a functional and physical interaction with T-antigen (Safak et al., 2001). Mapping studies found that the region of agnoprotein that interacts with T-antigen is localized to its amino-terminal half while the region of T-antigen that is involved in the interaction is localized to its central portion. Similarly agnoprotein is able to functionally interact with the cellular transcription factor YB-1 and negatively regulate YB-1-mediated activation of the JCV early and late promoters (Safak et al., 2002).

Interestingly agnoprotein can exert profound effects on cells when it is expressed in the absence of the other viral proteins. NIH-3T3 mouse fibroblasts that constitutively expressed JCV agnoprotein showed dysregulation of cell cycle progression and accumulated at the G_2/M phase (Darbinyan et al., 2002). Concomitantly, a decline in cyclins A- and B-associated kinase activity was observed in these cells. Agnoprotein showed the ability to augment the activity of the p21/WAF-1 promoter and increased the level of p21/WAF-1 protein in cells. In addition, agnoprotein was shown to bind p53. Activation of p21/WAF-1 gene expression in cells expressing agnoprotein may be mediated, at least in part, through cooperation with p53 (Darbinyan et al., 2002). Results from a p53 null cell line revealed that agnoprotein can induce p21/WAF-1 transcription but to a much lesser extent than in p53-expressing cells indicating the existence of a p53-independent mechanism for p21/WAF-1 activation by agnoprotein (Darbinyan et al., 2002).

Agnoprotein expression also has effects on the response of cells to DNA damage. Cells expressing ectopic agnoprotein were more sensitive to the cytotoxic effects of cisplatin and exhibited increased chromosome fragmentation and micronuclei formation (Darbinyan et al., 2004). Under conditions where moderate chromosome damage was observed in control cells, severe chromosomal pulverization was seen in agnoprotein-expressing cells. Non-homologous end joining is a major mechanism of double strand DNA break repair and is impaired in nuclear extracts from cells that express agnoprotein. This appears to be due to agnoprotein binding to the Ku70 DNA repair protein and sequestering it in the perinuclear space. Indeed, in vitro synthesized agnoprotein could directly bind to Ku70 in cell extracts and inhibit non-homologous end joining (Darbinyan et al., 2004). Agnoprotein also impaired DNA damage-induced cell cycle arrest.

The inhibition of DNA repair that is exerted by JCV agnoprotein is a likely contributor to the well-documented genomic instability conferred on cells when they undergo polyomavirus infection. This has a number of biological ramifications. Firstly, in a restrictive setting, polyomavirus gene expression may contribute to the progression of cells to a malignant phenotype (reviewed recently in White and Khalili, 2004a,b). Secondly, during lytic infections by JCV such as occur in PML, changes to the host glial cells may occur that are conducive to JCV propagation. These changes may be responsible for histopathological features of PML such as bizarre astrocytes and intranuclear oligodendrocyte inclusion bodies.